U.PORTO

MASTER'S DEGREE
NEUROBIOLOGY

Exploring the SNpL-Striatal Circuitry of Hyperacusis and Avoidance Behaviours in a Mouse Model of Autism

Luís Castro Fernandes Benge

M

2026

FACULTY OF MEDICINE OF THE UNIVERSITY OF PORTO

EXPLORING THE SNpL-STRIATAL CIRCUITRY OF HYPERACUSIS AND AVOIDANCE BEHAVIOURS IN A MOUSE MODEL OF AUTISM

Luís Castro Fernandes Benge





MASTER'S DEGREE IN NEUROBIOLOGY

SUPERVISOR: Professor Patrícia Monteiro
CO-SUPERVISOR: Dr. Sara Reis

2026

FUNDING

This project was funded by the FCT projects 2022.05228.PTDC, 2024.17843.PEX and 2024.16361.PEX; as well as COMPETE2030-FEDER-2023.17917.ICDT-15968.

ACKNOWLEDGMENTS

I'll start this thesis by expressing my sincere gratitude to the people that taught me what I've learnt throughout this year and that have helped me along the way when I felt lost. First, I'm thanking Professor Patrícia Monteiro for taking me in the lab and taking the role as my supervisor. I extend this gratefulness to my co-supervisor, Dr. Sara Reis not only for all the coding and algorithmic development entailed in this study, as well as the proper injections I could not do myself, but also for all the knowledge passed down to me, the perfect balance between the calming words and the assertive tone I needed in the right moments, and for being there for all the hand holding throughout. I'll also thank all my labmates but particularly Dr. Liliana Luz, Carolina Castro, and Alexandra Cruz for teaching me the foundational techniques in genotyping and western blotting, as well as all the venting sessions with an amazing soundtrack in the background.

Aos meus colegas neurocríticos™, obrigado por serem quem são e terem adicionado um lado tão bonito a este mestrado. Agradeço particularmente ao Guilherme, por ser o biólogo que respeito e que me acompanha seja no comboio ou no metro até ao planetário enquanto recebemos olhares julgadores; à Mafalda e ao Gonçalo por serem os labmates honorários fora de horas e local, e pelas sessões infindáveis de "Nem sabes..." à porta fechada; à Margaridenha por todo o apoio imensurável em tudo, por ter sido a pinga azul de companhia no mar amarelo em que a própria me meteu e pelas Ted Talks durante os jantares pré ensaio; a todo o GATU por me terem feito gostar tanto das segundas-feiras à noite e me terem feito sentir tão acolhido no único ano em que tive ao vosso lado. Não quero que passe despercebido o quanto significou para mim ter-vos a todos ao meu lado neste canto do Porto.

Em termos de palavras de apreço, deixo por escrito o maior obrigado que alguma vez poderei proferir ou relatar sem ser em latim ou com emojis a todos os que já me ouviram dizer que não se agradece. A QBQ, aos meus campeões e ao ano mais demente e desumilde de que já alguma vez se ouviu falar, obrigado por me ensinarem a "ser" quando "estar" não chega, e por fazerem com que um "adeus" custe tanto. Enfim, Leões, de vós me despeço.

Aos meus pais e aos meus irmãos, obrigado por fazerem de mim quem sou, por me fazerem crescer e se deixarem crescer a meu lado, pela companhia que me fazem quando acho que só quero estar sozinho, pela beleza que me fazem reconhecer no meio do caos e por tudo aquilo que não seja transmissível por palavras. Love you the most.

Tenho dito.

“Look, I made a hat, where there never was a hat.” – *Stephen Sondheim (Sunday in the Park with George*)

ABSTRACT

Autism Spectrum Disorder (ASD) is a neurodevelopmental disorder that affects over 61 million people worldwide and is marked by social-communication deficits, and repetitive behaviours. It's frequently accompanied by altered sensory reactivity (ASR), with decreased sound tolerance (DST) or hyperacusis among its most prevalent and debilitating manifestations, reported in up to 86% of autistic individuals. This DST can often lead to one's increased isolation by avoiding sound-associated environments thus compounding with pre-existing social difficulties. The neural circuitry linking hyperacusis to avoidance behaviours in ASD, however, remains to be elucidated. The auditory cortex relays the afferent auditory information to the tail of the striatum (TS), the caudal-most region of the striatum which, in turn is highly innervated by dopaminergic neurons of *the substantia nigra pars lateralis* (SNpL). In WT rodents, this circuit modulates auditory discrimination and attentional shift, and the balance between avoidance of aversive stimuli and threat overcoming behaviour via opposing D_1- and D_2-Receptor-expressing Striatal Projection Neurons (SPNs). Despite dopaminergic dysregulation having been reported as a feature of ASD, its involvement in this specific circuit in this context hasn't been examined. As such, this work aimed to determine whether the dopaminergic SNpL-TS circuit is altered in *Shank3*-InsG3680$^{(+/+)}$ knock-out (KO) mice, a genetic mouse model of ASD, and whether such alterations correlate to increased auditory avoidance. Viral tracing confirmed a direct SNpL-to-TS projection in the mouse brain, establishing the anatomical basis for this circuit. Building on this, an auditory looming paradigm was used and confirmed that *Shank3* KO mice display an auditory avoidant phenotype not dependent on anxiety- or locomotion-related variables. To investigate whether this phenotype could be explained by dopaminergic dysfunction within the circuit, preliminary levels of tyrosine hydroxylase (TH), the rate-limiting enzyme in dopamine synthesis, were assessed but showed no significant genotype differences in either the *substantia nigra* or the TS. Preliminary fluorescence data further suggested a trend towards reduced D_1-Receptor expression in *Shank3* KO mice in both the TS and SNpL, prompting a functional test of dopaminergic receptor involvement. However, systemic administration of a D_2- receptor agonist, pramipexole, reduced exploratory entries in the auditory looming paradigm due to a non-specific sedative effect.

Together, these findings support the *Shank3*-InsG3680$^{(+/+)}$ model as displaying a reliable auditory avoidance phenotype, while the preliminary dopaminergic findings highlight the need for further investigation into the mechanism underlying this behaviour.

Keywords: Autism Spectrum Disorder (ASD), Hyperacusis, Tail of the Striatum, *Substantia Nigra pars Lateralis* (SNpL), Avoidance Behaviours, Dopamine

RESUMO

A Perturbação do Espectro do Autismo (PEA) é uma perturbação a nível de neurodesenvolvimento que afeta mais de 61 milhões de pessoas mundialmente e é caracterizada por défices em comunicação social e comportamentos repetitivos. É frequentemente acompanhada por uma alteração na reatividade sensorial, sendo a diminuição da tolerância ao som (DTS), ou hiperacusia, uma das suas manifestações mais prevalentes e debilitantes, reportada em até 86% de indivíduos autistas. Esta DTS pode conduzir a um maior isolamento através da evitação de ambientes com estimulação sonora, agravando assim as dificuldades sociais pré-existentes. Contudo, o circuito neuronal que liga a hiperacusia aos comportamentos de evitação na PEA ainda está por elucidar. O córtex auditivo transmite a informação auditiva aferente à cauda do estriado (TS), a região mais caudal do corpo estriado que, por sua vez, é densamente inervada por neurónios dopaminérgicos da *substantia nigra pars lateralis* (SNpL). Em roedores wild-type (WT), este circuito modula a discriminação auditiva e foco de atenção, bem como o equilíbrio entre a evitação de estímulos aversivos e a superação de uma ameaça, através de populações neuronais opostas de neurónios do estriado de projeção (SPNs) que expressam recetores dopaminérgicos D_1 e D_2. Apesar da desregulação dopaminérgica já ter sido reportada como uma característica da PEA, o seu envolvimento neste circuito específico, e neste contexto, ainda não foi examinado. Como tal, este trabalho teve como objetivo determinar se o circuito dopaminérgico SNpL-TS se encontra alterado num modelo genético de murganho de PEA, *Shank3*-InsG3680$^{(+/+)}$, e se essas alterações apresentam alguma correlação com um aumento da evitação de estímulos auditivos. Técnicas de viral tracing confirmaram uma projeção direta da SNpL para a TS no cérebro de murganho, estabelecendo uma base anatómica para este circuito. Daí, um paradigma de looming auditivo foi usado que confirmou um fenótipo de evitação auditiva em murganhos *Shank3* KO, sem atribuição a variáveis relacionadas com ansiedade ou locomoção. Para verificar se este fenótipo poderia ser explicado por disfunções dopaminérgicas no circuito mencionado, níveis preliminares de tirosina hidroxilase (TH), a enzima limitante da velocidade de síntese da dopamina, foram medidos, mas não mostraram diferenças significativas entre genótipos, quer na *substantia nigra* quer na TS. Dados preliminares de fluorescência sugeriram ainda uma tendência para uma expressão reduzida dos recetores D_1 em murganhos *Shank3* KO, tanto na TS como na SNpL, levando a testes funcionais do envolvimento dos recetores dopaminérgicos. Porém, administração sistémica de um agonista dos recetores D_2, o pramipexol, reduziu as entradas na região de som no paradigma de looming auditivo devido a um efeito sedativo geral. Em conjunto, estes resultados reforçam o modelo *Shank3*-InsG3680$^{(+/+)}$ como tendo um fenótipo de evitação auditiva enquanto os resultados dopaminérgicos realçam a necessidade de mais investigação sobre os mecanismos envolvidos nestes comportamentos.

Palavras-chave: Perturbação do Espetro de Autismo, Hiperacusia, Cauda do Corpo Estriado, *Substantia Nigra pars Lateralis* (SNpL), Comportamentos de Evitação, Dopamina

TABLE OF CONTENTS

LIST OF ABBREVIATIONS....xiii

LIST OF FIGURES....xv

LIST OF TABLES....xvii

1 | INTRODUCTION....1

1.1 Autism Spectrum Disorders (ASD)....3
1.1.1 History, diagnostics, and aetiology....3
1.1.2 Altered sensory reactivity (ASR)....4
1.2 Sound Processing in ASD and Hyperacusis....6
1.2.1 Ascending auditory pathway....6
1.2.2 Mechanisms of hyperacusis....9
1.3 Coordination of Avoidance Behaviours....10
1.3.1 Classical measures of avoidance....10
1.3.2 Basal Nuclei in avoidance: the Tail of the Striatum (TS)....11
1.4 A Dopamine Overview....15
1.4.1 Synthesis, transmission, and termination....15
1.4.2 Subregional dopamine signalling in the TS....16
1.4.3 The dopamine system in ASD....17
1.5 The End Goal....18
1.5.1 Animal model of ASD: *Shank3* KO mice....18
1.5.2 Hypothesis and Objectives....19

2 | MATERIALS AND METHODS....21

2.1 Animal Model....23

2.2 Genotyping....23

2.3 Stereotaxic Injections....24

2.4 Behavioural Tests....25

2.4.1 Auditory Looming Paradigm....25

2.4.2 Homecage test....25

2.4.3 Behavioural Analysis....26

2.5 Western Blots....26

2.5.1 Protein extraction and quantification....26

2.5.2 SDS-PAGE....27

2.5.3 Immunoblotting....27

2.6 Immunohistochemistry (IHC)..... 28

2.7 Image acquisition and analysis..... 29

2.8 Statistical Analysis..... 29

3 | RESULTS.....31

3.1 The SNpL-Striatal Circuitry is Confirmed in Mice.....33

3.2 *Shank3* KO Mice Show Increased Avoidance Behaviours to Auditory Looming Stimuli..... 34

3.3 Tyrosine Hydroxylase Levels Seem Unaltered Between Genotypes..... 36

3.4 D_1Rs May Be Less Expressed in Neurons of *Shank3* KO Mice Than in WT Mice...38

3.5 Administration of D2R Agonists Lowers Overall Movement.....39

4 | DISCUSSION..... 43

4.1 The *Shank3*-InsG3680$^{(+/+)}$ Mouse Model Shows Auditory Avoidance in More Than One Way.....45

4.2 Tyrosine Hydroxylase Levels Don't Support a Dopamine Synthesis Increase in The SNpL or the TS of *Shank3* KOs.....46

4.3 Dopaminergic Action May Be Altered at a Receptor Level in *Shank3* KO Mice...47

4.4 Dopamine Clearance Mechanisms Remain Unexplored.....49

5 | FINAL REMARKS.....51

5.1 Limitations.....53

5.2 Future Perspectives.....55

REFERENCES..... 57

LIST OF ABBREVIATIONS

6-OHDA – 6-Hydroxydopamine

AADC – Aromatic L-amino acid decarboxylase

AAV – Adeno-associated Virus

ABR – Auditory Brainstem Response

AC – Auditory Cortex

aCSF – Artificial Cerebrospinal Fluid

AP – Anteroposterior

APS – Ammonium Persulfate

ASD – Autism Spectrum Disorders

ASR – Altered Sensory Reactivity

BCA – Bicinchoninic Acid

BSA – Bovine Serum Albumin

cAMP – Cyclic adenosine monophosphate

CNTNAP2 – Contactin-associated protein-like 2

CN VIII – 8th Cranial Nerve

COMT – Catechol-O-Methyltransferase

cp – Cerebral Peduncle

CPu – Caudate Putamen

CS – Conditional Stimulus

D_1R – Dopamine Receptor D_1

D_2R – Dopamine Receptor D_2

DA – Dopamine

DAPI – 4',6-diamidino-2-phenylindole

DAT – Dopamine Transporter

DβH – Dopamine β-Hydroxylase

DEGs – Differentially Expressed Genes

DGAV – Direção-Geral da Alimentação e Veterinária

DIO – Double-floxed Inverted Orientation

DNA – Deoxyribonucleic Acid

DRN – Dorsal Raphe Nucleus

DSM – Diagnostic and Statistical Manual of Mental Disorders

DV – Dorsoventral

E/I – Excitatory/Inhibitory

ECL – Enhanced Chemiluminescence

eGFP – Enhanced Green Fluorescent Protein

ERP – Event-related Potentials

FrA – Frontal Association Cortex

FSCV – Fast Scan Cyclic Voltammetry

GABA – γ-aminobutyric Acid

GAD – Glutamate Decarboxylase

GP – *Globus Pallidus*

GPe – External *Globus Pallidus*

Gpi – Internal *Globus Pallidus*

HRP – Horseradish Peroxidase

IC – *Inferior Colliculus*

ic – Internal Capsule

IHC – Immunohistochemistry

InC – Insular Cortex

KO – Knock-out

LDL – Loudness Discomfort Level

L-DOPA – Levodopa

LP – Lateral Posterior thalamic Nuclei

LV – Lateral Ventricle

MAO – Monoamine Oxidase

MD – Mediodorsal thalamic Nuclei

MeCP2 – Methyl-CpG binding protein

MGN – Medial Geniculate Nuclei

ML – Mediolateral

MoC – Motor Cortex

MRI – Magnetic Resonance Imaging

OCT – Optimal Cutting Temperature

P10 – Postnatal day 10

PBS – Phosphate Buffer Saline

PCR – Polymerase Chain Reaction

PET – Positron Emission Tomographic

PFA – Paraformaldehyde

PIL – Posterior Intralaminar thalamic nuclei

PMS – Phelan-McDermid Syndrome

PNMT – Phenylethanolamine N-Methyltransferase

PPI – Prepulse Inhibition

rAAV – Retrograde Adeno-associated Virus

Rhi – Rhinal Cortices

RIPA – Radioimmunoprecipitation Assay

RNA – Ribonucleic Acid

ROI – Region of Interest

RRBs – Restricted Repetitive Behaviours

RT – Room Temperature

SC – Somatosensory Cortex

SDS – Sodium Dodecyl Sulphate

SEM – Standard Error of Mean

SHANK – SH3 and multiple Ankyrin repeat domains

siRNA – Small Interfering RNA

SN – *Substantia Nigra*

SNc – *Substantia Nigra pars Compacta*

SNpL – *Substantia Nigra pars Lateralis*

SNr – *Substantia Nigra pars Reticulata*

SOC – Superior Olivary Complex

SPF – Subparafascicular thalamic nucleus

SPNs – Striatal Projection Neurons

STN – Subthalamic Nucleus

TAE – Tris-Acetate-EDTA

TeA – Temporal Association Cortex

TEMED – Tetramethylethylenediamine

TH – Tyrosine Hydroxylase

TS – Tail of Striatum

VC – Visual Cortex

VP – Ventral Posterior thalamic nuclei

WB – Western Blot

WT – Wild Type

LIST OF FIGURES

Figure 1 | Graphic overview of the ascending auditory pathway. After transduction in the cochlea, auditory signals are carried by the vestibulocochlear nerve (CN VIII) to the cochlear nuclei in the brainstem and relayed sequentially through the superior olivary complex, the lateral lemniscus, the inferior colliculus, and the medial geniculate nucleus of the thalamus before reaching the auditory cortex. The blue lines trace the major ascending projections but several bilateral and crossed connections present at each level have been omitted for simplicity. Schematic, not to scale.....**7**

Figure 2 | General schematic of Basal Nuclei direct and indirect pathways. The cerebral cortex sends glutamatergic (excitatory) projections to the striatum. From there, two pathways modulate the output nuclei: the direct pathway (left) projects onto the GPi and SNr with an inhibitory signal, which facilitates movement by disinhibiting the signal relayed to the thalamus; the indirect pathway (right) relays GABAergic signals through the GPe and STN, the latter providing glutamatergic excitation onto the output nuclei, suppressing movement by potentiating the inhibitory synapses from the output nuclei to the thalamus. The thalamus sends excitatory projections back to the cortex, closing the loop and allowing for fine movement regulation.....**12**

Figure 3 | Schematic summary of the TS's connectivity. Coronal schematics of the mouse brain as a summary of input and output pathways of the TS (cyan). Inputs (yellow) stem from a broad set of sensory and association cortices, as well as subcortical and thalamic nuclei. Monoaminergic inputs (blue) arise from the SNpL for the case of dopamine and the DRN for serotonin. TS outputs are presented in a cell-type dependent segregation with direct-pathway D_1R-SPNs (green) projecting to the GPi and SNr and the indirect-pathway D_2R-SPNs (red) projecting to the GPe. Abbreviations: AC, Auditory Cortex; DRN, Dorsal Raphe Nucleus; FrA, Frontal Association Cortex; GPe, external *Globus Pallidus*; GPi, internal *Globus Pallidus*; InC, Insular Cortex; LP, Lateral Posterior Nuclei; MD, Mediodorsal Nuclei; MG, Medial Geniculate Nucleus; MoC, Motor Cortex; PIL, Posterior Intralaminar Nucleus; Rhi, Rhinal Cortices (ecto-, endo-, peri-); SC, Somatosensory Cortex; SNpL, *Substantia Nigra pars Lateralis*; SNr, *Substantia Nigra pars Reticulata*; TeA, Temporal Association Cortex; VC, Visual Cortex; VP, Ventral Posterior nuclei.....**13**

Figure 4 | Dopamine synthesis and metabolism pathways. L-tyrosine is converted to L-DOPA by the TH enzyme. L-DOPA is converted to dopamine by the AADC enzyme. Dopamine can be metabolised into norepinephrine by the DβH enzyme. Norepinephrine is converted to epinephrine by the PNMT enzyme.....**15**

Figure 5 | Graphic summary of viruses and coordinates considered for stereotaxic surgery to target the TS and the SNpL. Schematic injection layout in coronal slices of a mouse brain with the TS and SNpL regions highlighted.....**24**

Figure 6 | SNpL neurons show an established projection to the TS. a. Stereotaxic bilateral injection of retrograde rAAV-Cre virus into TS and AAV5-DIO-eGFP into SNpL. **b.** Representative immunofluorescent image of a horizontal brain section of a mouse brain with eGFP in green and TH-stained cells in red. Abbreviations: CPu, Caudate *Putamen*; GPe, external *Globus Pallidus*; IC, Internal Capsule; LV, Lateral Ventricle; SNpL, *Substantia Nigra pars Lateralis*; SPF, Subparafascicular thalamic nucleus.....**33**

Figure 7 | *Shank3* KO mice enter the auditory looming region less often than WT mice while showcasing negligible differences in the time spent in their nests and travelled distance. a. Diagram of Auditory Looming paradigm: Individual mice are placed in an open arena with a small piece of their nest in the corner (bottom left). After a habituation period of 3 minutes, a 10-minute stimulation period ensues in which a crescendo auditory stimulus starts playing upon the animal's entrance in a designated region of interest (ROI) (dotted rectangle) **b.** Number of times each WT and KO mouse entered the ROI during their trial of auditory looming behavioural test. **c.** Percentage of time each WT and KO mouse spent in their nest during each period of their trial of auditory looming behavioural test. **d.** Distance travelled within the arena by each WT and KO mouse during each period of their trial of auditory looming behavioural test. Values presented as mean ± SEM. ns – no significant difference. *p < 0.05. *(WT: n = 9 mice; KO: n = 9 mice)*.....**35**

Figure 8 | Immunohistochemical staining of TH in the SN suggests slightly lower levels in *Shank3* KO mice but western blot data shows no differences. a. Representative immunofluorescent images from coronal brain sections of WT (above) and KO (below) mice staining nuclei in blue and TH in green in the SN with 20x objective lens. **b.** Number of TH-expressing cell bodies normalised for total number of DAPI nuclei in SNpL. *(WT: n = 2 mice; KO: n = 4 mice)* **c and d.** Western Blot results. Representative Western Blot of TH and β-actin bands in WT (left) and KO (right) brain tissue from the SN (**d.**) and quantification of TH signal normalised for β-actin (**c.**). *(WT: n = 7 mice; KO: n = 6 mice)*. Values presented as mean ± SEM. ns – no significant difference. Abbreviations: cp, cerebral peduncle; SNc, *Substantia Nigra pars Compacta*; SNpL, *Substantia Nigra pars Lateralis*; SNr, *Substantia Nigra pars Reticulata*.....**36**

Figure 9 | Immunohistochemical staining of TH in the TS suggests a slight increase in *Shank3* KO mice but western blot data show no difference. a. Representative immunofluorescent images of coronal brain sections from WT (left) and KO (right) mice staining nuclei in blue and TH in green in the TS with 20x objective lens. **b.** Measured signal intensity of TH normalised for total area of TS. *(WT: n = 2 mice; KO: n = 4 mice)*. **c and d. Western Blot results.** Representative Western Blot of TH and β-actin bands in WT (left) and KO (right) brain tissue from the TS (**d.**) and quantification of TH signal normalised for β-actin (**c.**). *(WT: n = 7 mice; KO: n = 6 mice)*. Values presented as mean ± SEM. ns – no significant difference. Abbreviations: GPe, external *Globus Pallidus; TS, Tail of the Striatum*.....**37**

Figure 10 | Expression of tdTomato in the TS and SNpL suggests lower levels of D_1R in *Shank3* KO mice compared to WT mice. a. Representative images of coronal brain sections from WT (left) and KO (right) mice, showing DAPI staining in blue and D_1R-tdTomato signal in red in the TS with 20x objective lens. **b.** Number of D_1R-tdTomato-expressing cell bodies normalised for total number of DAPI nuclei in the TS. *(WT: n = 2 mice; KO: n = 2 mice)*. **c.** Representative images of coronal brain sections from WT (above) and KO (below) mice, showing DAPI staining in blue and D_1R-tdTomato signal in red in the SN with 20x objective lens. **d.** Measured signal intensity of D_1R-tdTomato normalised for total area of SNpL. *(WT: n = 2 mice; KO: n = 2 mice)*. Values presented as mean ± SEM. Abbreviations: cp, cerebral peduncle; GPe, external *Globus Pallidus*; SNpc, *Substantia Nigra pars Compacta*; SNpL, *Substantia Nigra pars Lateralis*; SNr, *Substantia Nigra pars Reticulata; TS, Tail of the Striatum*.....**38**

Figure 11 | Pramipexole-injected mice enter the sound area less often than saline injected mice and spend more time in the nest regardless of genotype. a. Number of times each WT and KO mouse entered the ROI during their trial of auditory looming behavioural test after being injected intraperitoneally with saline solution (left) *(WT: n = 2 mice; KO: n = 2 mice)* or D_2R agonist, pramipexole (right) *(WT: n = 4 mice; KO: n = 4 mice)*. **b.** Percentage of time each WT and KO mouse spent in their nest during each period of their trial of auditory looming behavioural test after being injected intraperitoneally with saline solution (left) *(WT: n = 2 mice; KO: n = 2 mice)* or D_2R agonist, pramipexole (right) *(WT: n = 4 mice; KO: n = 4 mice)*. Values presented as mean ± SEM.....**39**

Figure 12 | Pramipexole-injected mice move less than saline-injected mice in home-cage test with no triggerable auditory stimulus. a. Diagram of home cage behavioural recording. Mice are placed in their original housing cages with their housing mates for 10 minutes while being recorded. **b.** Amount of time each individual mouse spent moving inside the cage after being injected intraperitoneally with saline solution *(WT: n = 2 mice; KO: n = 2 mice)* or D_2R agonist, pramipexole *(WT: n = 5 mice; KO: n = 5 mice)*. Values presented as mean ± SEM.....**40**

LIST OF TABLES

Table 1 | Primer sequences and PCR conditions for genotyping of *Shank3*-InsG3680$^{+/+}$.....**23**

Table 2 | Primary and secondary antibodies used for immunoblotting.....**28**

Introduction

- *AUTISM SPECTRUM DISORDERS (ASD)*
- *SOUND PROCESSING IN ASD AND HYPERACUSIS*
- *COORDINATION OF AVOIDANCE BEHAVIOURS*
- *A DOPAMINE OVERVIEW*
- *THE END GOAL*

1 | INTRODUCTION

1.1 Autism Spectrum Disorders (ASD)

1.1.1. History, diagnostics, and aetiology

In 1911, Swiss psychiatrist Eugen Bleuler coins the term "autism" for the first time to describe a symptom of self-detachment from reality in schizophrenia[1], and until the 1940s the two terms remain conceptually intertwined, later being adopted by Austrian-American psychiatrist Leo Kanner in his account of children exhibiting a disturbance of affective contact. From that account, a more discriminatory report emerges, giving rise to what is conventionally treated as the foundational clinical description for modern autism[2] and culminating with the publishing of the third edition of the Diagnostic and Statistical Manual of Mental Disorders (DSM-III) in 1980, officially introducing "Infantile Autism" as a developmental disorder distinct from schizophrenia defined by its own specific behavioural criteria[3]. Years later, the fourth edition of the DSM (DSM-IV (1994)) becomes the first to formally recognise and organise autism as a spectrum comprising five related but individual diagnoses[4], finally leading to the DSM-5 (2013), which consolidates the previously separate diagnoses into a single, all-encompassing one as autism spectrum disorders, now defined along two core symptom categories instead of by discrete subtypes[5].

The most recent edition of the DSM (DSM-5-TR (2022)), states that a diagnosis of ASD must note the simultaneous manifestation of multiple criteria, those being, in crude summary, (A) persistent deficits in social communication; (B) restricted, repetitive patterns of behaviour (RRBs); (C) presence of symptoms from childhood; (D) clinically significant impairment in areas of functioning directly caused by the symptoms; (E) symptoms can't be better explained by intellectual disability or global developmental delay alone. Despite the comprehensive criteria list for diagnosis, there is no "one-size-fits-all" definition, as, as indicated by the word "spectrum", it presents with substantial variation in presentation and support needed across one's lifespan with different autistic individuals differing in intellectual functioning, and co-occurring conditions, meaning that two people given the same diagnostic may present very differently[6].

Estimates regarding ASD's prevalence have risen sharply since the 1990s, in large part due to broadened diagnostic criteria, increased clinical and societal awareness, and overall wider access to proper assessment[7,8]. The Centres for Disease Control and Prevention's Autism and Developmental Disabilities Monitoring network had a recorded ASD prevalence in the United States of roughly 1 in 150 eight-year-old children in the year 2000, but by 2022 this figure had risen to approximately 1 in 31 children for the same age group (3.2%), with a notably larger incidence in boys[9]. This sexual dimorphism has been consistently present in epidemiological studies done in ASD, with a higher prevalence of

diagnosis in males than in females at an average ratio of 3:1, 4:1, or even 5:1 depending on the methodology used by the various studies and the age groups included[10–12].

Despite ASD's growing incidence, its aetiology is nonetheless heterogeneous in nature with no attributable pinpointed cause or explanation and research suggesting that it may stem from both environmental and genetic factors[13]. While pre-, peri-, and postnatal environmental factors (such as advanced maternal or paternal age (≥ 35 years), maternal nutritional intake and medicinal use of drugs such as valproic acid and thalidomide), and maternal immune response[14], show a strong association to ASD diagnosis in offspring, studies done in twins and families place heritability estimates between 64 and 91% indicating a substantial genetic impact as a risk factor[15]. Regarding genetic studies surrounding ASD, one of the largest-scale whole-exome sequence analysis conducted with 35584 biological samples has distinguished 102 ASD-associated genes#. Of those genes, multiomic and functional research tends to converge in reported changes to genes involved in core pathways in ASD biological samples, such as chromatin remodelling (e.g. the *CHD8* and *ARID1B* genes[16–18]), protein regulation (e.g. the *FMR1* and *PTEN* genes[22,23]), or synaptic scaffolding (e.g. the *NRXNs* and *SHANKs* genes[24–26]). Multiple differentially expressed genes (DEGs) have been identified in ASD[27] and when recreated and studied in mutant animal models, have allowed for a better understanding of their downstream roles. The fragile X mental retardation protein (FMRP), for example, is an RNA-binding protein encoded by the *Fmr1* gene involved in protein regulation at the synaptic level by modulating mRNA translation#. Research conducted in *Fmr1* KO mice models alone, has reproduced some of the most generally backed up mechanisms thought to be implied in its pathogenesis, like compromised synaptic integrity[28], imbalanced excitatory/inhibitory (E/I) dynamics[29,30], or dysregulated neurotransmitter systems[31]. This *Fmr1* KO has also resulted in the mutant mice displaying certain behavioural phenotypes like impaired social interactions, repetitive behaviours, and atypical sensory reactivity, further enlightening the genetic role played in ASD's aetiology.

Even so, with the heterogeneity implied and consistently verified of symptoms and severity in people with ASD, no genetic or environmental factor has been successfully singled-out as a pathognomonic sign for this disorder.

1.1.2. Altered sensory reactivity (ASR)

Regardless of its diverse aetiology, ASD is commonly referred to as a neurodevelopmental disorder surrounding its two core symptom categories. Although criteria A and B are both necessarily present in all people with ASD, each domain presents different day-to-day difficulties among the affected population.

Criterion A encompasses the socialising domain hardships involved, demanding simultaneous reported deficits in social-emotional reciprocity, in nonverbal communicative behaviours like eye contact and body language, and in development, maintenance, and understanding of relationships, currently or by history[6]. Its implied afflictions emerge in literature as reported estimates of 40% of autistic adults lacking reciprocal friendships[32], or 34% of autistic people being employed compared to roughly 54% of people with disabilities or 83% of people without disabilities[33]. These poor outcomes are consistently associated with poorer mental health and lower quality of life across the lifespan but, notably, can't be attributed to cognitive impairments as they persist even among autistic people with average- to above-average intelligence[34].

As for criterion B, it deals with RRBs and only requires reports of two patterns among stereotyped/repetitive motor movements, object use, or speech (stimming); insistence on sameness or inflexible routines; highly restricted, fixated interests; and hyper- or hypo-reactivity to sensory input or unusual sensory interest, currently or by history[6]. These behaviours have more directly observable complications as certain manifestations present in self-injurious behaviour[35] and active social isolation[36], but RRBs severity is also highly and adversely associated with development of language and communication, as well as social functioning[37,38], feeding into the problems previously covered in criterion A.

Particularly, of the criterion B patterns, ASR didn't show up as part of any criteria prior to the DSM-5 and it was only added after research repeatedly confirmed the widespread effect it had, with current reports stating its presence in over 90% of autistic people[39]. ASR affects individuals with ASD across all sensory modalities and can be manifested differently in behaviour either through an exaggerated or dampened response to a given stimulus or through an unusual interest towards it. Moreover, sensory problems in ASD have been associated with anxiety, self-injurious behaviours, sleep disturbances and more, having been reported as directly affecting regular daily functioning. A frequently used model for the classification of sensory characteristics in ASD is Dunn's four quadrant model which aligns sensory processing along two axis, those being neurological thresholds which range from low to high depending on neural responses to sensory stimuli, and behavioural responses which range from passive to active depending on the elicited responsive strategy towards a given stimulus. Together, these two axes establish this model's four quadrants, helping the categorisation of sensory processing.

Visually, patients with ASD have been documented to showcase hypersensitivity to flashing lights, heightened sensory responses to stimuli in the visual periphery, and enhanced detail perception which has been proposed to contribute to perceptual overload in day-to-day scenarios. Autistic individuals have also been reported as displaying lower contrast sensitivity to both moving and unmoving stimuli, though in this domain different studies found no difference between the ASD and the neurotypical groups. Tactile alterations have also been reported in ASD as manifested through hyperreactivity to thermal stimuli or light touches in instances like grooming, though contradicting results

emerge on the latter in a study considering ASD adults. Auditory alterations have likewise been documented in literature and will be discussed further in this work, but tests pertaining to audition have been particularly useful to showcase how, on top of its widespread prevalence, ASR is also detectable very early in development. Findings regarding methodologies such as auditory brainstem responses (ABR) assessed by measuring auditory stimulus-evoked electrical activity in the vestibulocochlear nerve and brainstem have revealed longer latencies in neonatal babies who are later diagnosed with ASD[40] as well as children presenting reduced prepulse inhibition (PPI)[41] thus indicating lower sensory gating to repeated sounds, making the case for its lifelong effects in patients.

1.2 Sound processing in ASD and Hyperacusis

Of the classically described five senses, hearing rises as a particularly and recurringly affected one in ASD[42] with a particular directional bias towards hyperreactivity that often results in strong aversive reactions to sound or an overall decreased sound tolerance[43] (DST). DST usually serves as an umbrella term encompassing more specific but distinct sound-related ailments that revolve around different manifestations of hyperacusis. As proposed by Tyler and colleagues#, these manifestations are conventionally separated into loudness, pain, annoyance (approximately corresponding to misophonia), and fear (approximately corresponding to phonophobia). Hyperacusis in autism has been described as one of the disorder's most debilitating sensory features[44], having been reported in as much as 86% of people with ASD at least once in their lifetime, as compared to <20% in neurotypical people[43,45] .

1.2.1 Ascending auditory pathway

For a proper discussion of the mechanisms of hyperacusis, it's important to understand how sound is processed in the first place.

Briefly, sound travels as air pressure waves that cause the tympanic membrane to vibrate, and these vibrations are transmitted through the middle ear ossicles to the cochlea. There, a mechanoreceptor population with stereocilia-projecting cells, converts the mechanical signal into electrochemical nerve impulses. These impulses are transmitted directly to the vestibulocochlear nerve and travel up to the cochlear nuclei which project to the superior olivary complex (SOC) in the brainstem, the first place where binaural information converges. From there, the stimulus is transmitted through the lateral lemniscus to the inferior colliculus (IC) which then relays the signal to the medial geniculate nuclei (MGN) in the thalamus. These subnuclei serve as an association and processing hub and finally relay the stimulus to the auditory cortex (AC) where conscious perception of sound takes place (Figure 1)[46].

The structures involved in this pathway become particularly relevant in the context of altered auditory perception when discussing some of the more objective psychoacoustic and electrophysiological methods used to study it that go beyond parent- and self-reports.

When compared to an age- and sex-matched group of neurotypical children along a categorical loudness scale and auditory dynamics range tests (established from the gap between each participant's quiet threshold and their loudness discomfort level (LDL) for pure tones), autistic children and adolescents have shown DST at lower intensity levels before reaching discomfort despite absolute hearing thresholds being similar between the two groups indicating that the exaggeration of loudness perception may not be happening at a peripheral, cochlear level.

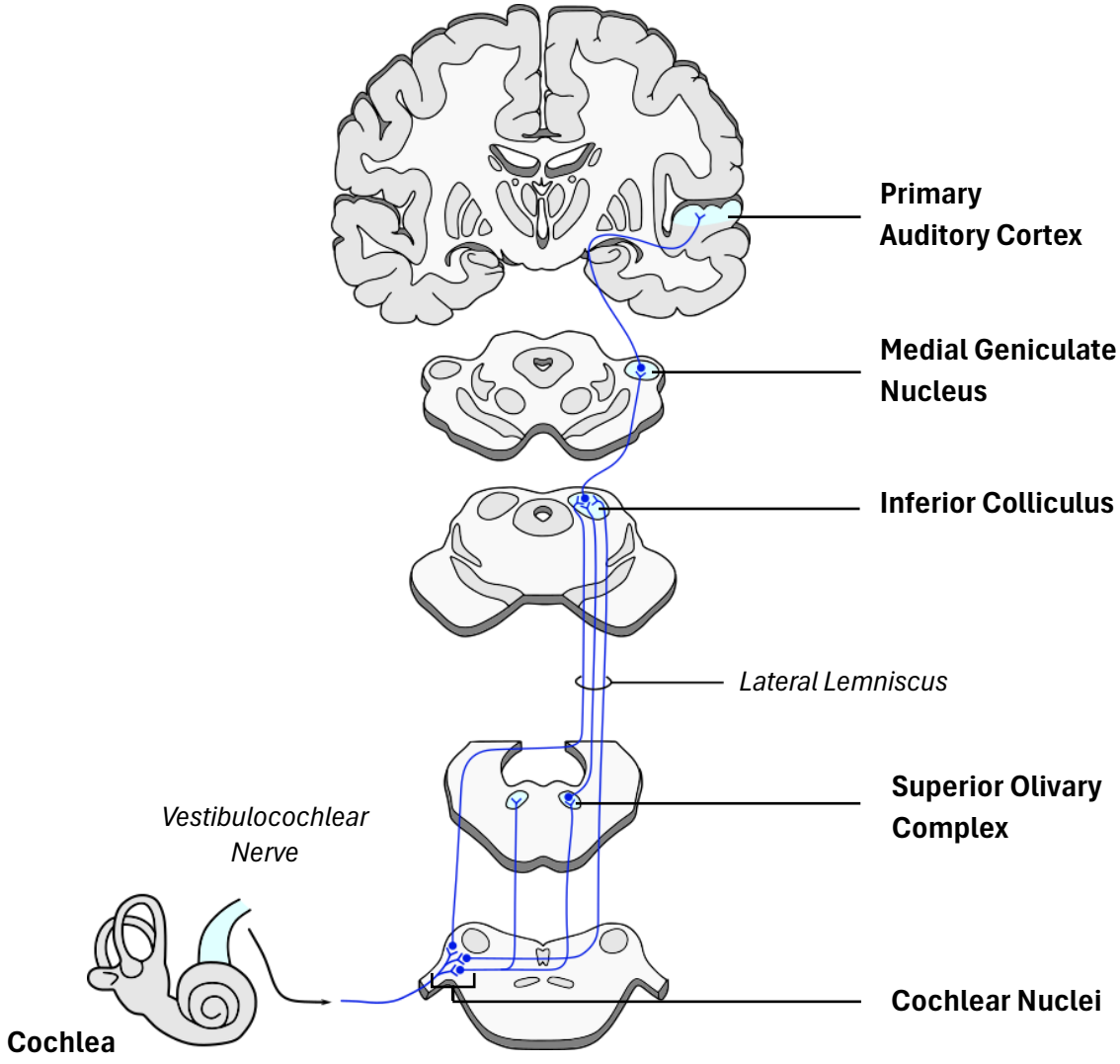


Figure 1 | Graphic overview of the ascending auditory pathway. After transduction in the cochlea, auditory signals are carried by the vestibulocochlear nerve (CN VIII) to the cochlear nuclei in the brainstem and relayed sequentially through the superior olivary complex, the lateral lemniscus, the inferior colliculus, and the medial geniculate nucleus of the thalamus before reaching the auditory cortex. The blue lines trace the major ascending projections but several bilateral and crossed connections present at each level have been omitted for simplicity. Schematic, not to scale.

At a more central level, altered auditory perception is also commonly assessed through other methods that don't rely on the test subject's spoken feedback, allowing for lab reproducibility in animal models.

As previously briefly described, the ABR measurements record sound-evoked potentials in a non-invasive manner through electrodes placed on the scalp. The recorded signal results in 5 sequential peaks (I-V) that translate synaptic relays from the CN VIII to the IC with peak I reflecting the signal in the CN VIII itself, peak II reflecting the cochlear nuclei, peak III reflecting the SOC, peak IV reflecting the lateral lemniscus, until reaching the IC as reflected by the signal observed in peak V. In ASD studies done in humans, the ABR measured in individuals younger than 18 years old show a prolonged latency in peaks III and V but, in studies conducted in adults, such latencies haven't been reported.

When recreated in animal models of autism, findings regarding the ABR show some level of heterogeneity depending on the model employed for the study. For example, the ABR's peak latency recovery from early age to childhood mentioned in humans has been documented in a *Cntnap2* KO rat model of autism with normal thresholds found to their ABR. However, the aforementioned *Fmr1* KO mouse model, has been shown to have a higher ABR threshold to the auditory stimuli presented while also presenting reduced wave amplitude in peaks I and III with no response or inter-peak latencies reported. Conversely, a transgenic *Mecp2*-overexpressing mouse model has had normal ABRs reported in spite of atypical responses having been documented further ahead in the auditory pathway, namely at a cortical level.

Another widely used assay is the measurement of the acoustic startle response by reflexive muscle contraction. The startle reflex measurements are often associated to its attenuation by prepulse inhibition (PPI) in which a weak auditory stimulus preceding a startle eliciting auditory stimulus is played, which allows to gauge any abnormalities in sensory gating. PPI has been found to be impaired in ASD patients, particularly amongst children and adolescent groups, reflecting reduced sensorimotor gating functions compared to neurotypical controls, but, among adults, those differences subside but, for this test, the results obtained across multiple animal models vary. While the *Fmr1* KO mouse model has been shown to present a reduced auditory startle reflex along with a more efficient PPI, for example, *Cntnap2* KO mice have had their acoustic startle reflex as well as their PPI documented as reduced, unchanged, and more efficient in different studies when compared to WT mice.

As for central processing assessment, *in vivo* electrophysiology measurements of activity through local field potentials, single-unit recordings, or event-related potentials (ERPs) allow for a more direct strategy, obtaining data pertaining to areas like the auditory cortex directly. Electroencephalography results in individuals with ASD have displayed altered auditory processing ability across multiple ERP components such as early sensory components like the P1 and N1, which are associated with auditory discrimination and

novelty and have shown reduced amplitude as well as delayed latency in ASD. Magnetoencephalography-measured ERP has also indicated altered auditory processing ability through the M100 component which arises as a result of an auditory evoked potential that happens 100ms after stimulus presentation and is associated with early sound perception and, in autistic individuals, has been reported with a consistent latency in the right hemisphere. This recurring latency in early sensory components has been documented with similar electrophysiological results in the P1 and N1 components in valproic acid-exposed mice models of autism.

These methods have allowed for progress to occur in the scope of DST by helping dissect crucial alterations in relay points in the auditory pathway but in spite of proposed mechanisms for overall hyperacusis, discriminatory approaches that explain its increased prevalence and downstream effects in the autistic community remain largely unexplored.

1.2.2 Mechanisms of hyperacusis

The underlying causes for hyperacusis are somewhat contested but the most widely accepted model points to excessive central auditory gain in which auditory stimuli are amplified in central areas of the auditory pathway by excessive neural activation of regions like the IC, the MGN and the AC as pointed out by MRI data, explaining why otherwise innocuous auditory stimuli can be perceived as debilitatingly loud[47,48].

Molecularly, the main explanations for this finding lie in reported alterations in the E/I balance with loss of inhibitory tone in brain regions involved in the ascending auditory pathway in animals with induced sensorineural hearing loss used as experimental models for hyperacusis[47]. In these animals, Glutamate Decarboxylase (GAD), responsible for the synthesis of GABA, has shown reduced expression levels in the AC and the IC, as well as lower levels of GABA receptors[49,50], emerging as a disinhibition of circuits that should attenuate perceived sound intensity.

The caveat is that, in this central auditory gain model used to study hyperacusis, the central gain increase is induced as a consequence of compromised cochlear activity but, despite mixed conclusions in research, hearing loss rates in ASD do not appear significantly higher than those in non-autistic people[51], and most of the people with ASD that present lower thresholds for loudness discomfort levels also show typically normal hearing thresholds[52], possibly signalling the existence of an alternative pathophysiological origin for hyperacusis. While these experiments help highlight the foundational issue of hyperacusis, no studies to date have directly compared its underlying mechanisms in neurotypical versus autistic brains. It therefore remains unclear whether hyperacusis arises through a distinct mechanism in ASD or reflects the same mechanism occurring at a higher prevalence in this population.

Proposed mechanistic explanations for central auditory gain in ASD preserve the idea of increased E/I ratio, similarly leading to an overactivation of the IC, the MGN, and/or the AC[44] especially as this feature is recurrently described in people with ASD in several different areas in the brain[53]. However, a specific model focusing on studying the hyperacusis in the context of ASD remains to be validated and used in future research.

1.3 Coordination of Avoidance Behaviours

1.3.1 Classical measures of avoidance

The harmful implications of hyperacusis go beyond the inherent discomfort it entails, often leading to self-withdrawal or active avoidance from loud environments and social contexts in the affected population[54], introducing an extra complication for day-to-day functioning in autistic people as it compounds with their previously mentioned problems socialising.

Auditory sensory stimuli influence motor actions in a plethora of ways but in the field of active avoidance and defensive behaviours, their influence is usually studied in the context of learnt avoidance paradigms, such as sound-cued fear conditioning, or innate avoidance behaviours, such as the acoustic startle reflex. These two categories recruit distinct neural pathways, with the acoustic startle reflex activating subcortical circuits that trigger motor responses before conscious perception occurs, whereas fear conditioning relies primarily on cortical and amygdalar processing[55,56].

The type of avoidance behaviour resulting from hyperacusis appears more like the former in nature despite emerging as a result of an innate condition for the case of ASD as autistic people learn to avoid environments where they expect sensory overload to be likely to occur[57]. One of the most popular ways to study avoidance behaviours is through adaptive sound-induced fear conditioning protocols but, as they employ a more Pavlovian-like approach in which the aversive outcome is independent of the subject's behaviour, these methods have proven more useful in studying the mechanisms behind the fear responses associated with the avoidance behaviours rather than the mechanisms that lead to the active avoidance behaviour per se. In these circumstances, the amygdala recurringly appears as a central part of the neural circuitry involved in forming the association between a stimulus and an aversive outcome, however, maintaining the learned avoidance response depends on the recruitment of other brain regions[58]. In the context of learnt avoidance behaviours specifically, these are more aptly studied in different paradigms that use aversive conditional stimuli (CS) that keep being produced until a given behaviour is displayed, leading to the animals being tested learning how to avoid the reoccurrence of said stimulus. From these experiments, the amygdala still appears active in the acquisition of the knowledge of the CS's perceived danger, but the motor response evoked from the

cortical perception of the stimuli seem to be gated by different subcortical structures in the basal nuclei[58].

1.3.2 Basal Nuclei in avoidance: the Tail of the Striatum (TS)

The Basal Nuclei are a collection of heterogeneous subcortical nuclei located in the brains of vertebrate animals mainly involved in the regulation of voluntary movements by modulating which ones get facilitated and which ones are suppressed. These nuclei also play key roles in habit formation, executive functions, action selection, procedural and conditional learning[59]. The components that comprise this structure are the caudate nucleus and the putamen (collectively referred to as the striatum), the globus pallidus (GP), the subthalamic nucleus (STN), and the *substantia nigra* (SN). These nuclei can be functionally grouped as input nuclei (striatum), which receive afferent information from cortical and thalamic structures; the output nuclei (internal *globus pallidus* (GPi), and substantia nigra pars reticulata (SNr)), which send out basal nuclei information to thalamic structures; and the intrinsic nuclei (STN, external *globus pallidus* (GPe), and substantia nigra pars compacta (SNc)), which relay information between the input and output nuclei[59]. The SNr has been shown to be the main output nucleus to gate active avoidance behaviours in CS paradigm studies, with upstream regulation of this structure happening at the striatal level through a direct, inhibitory pathway, or an indirect, excitatory pathway that is relayed by the intrinsic nuclei[58] (Figure 2).

In the context of sound processing and as the main gateway of the basal nuclei[60], the striatum (specifically its caudal-most part further discussed below) is the direct point of contact between the auditory cortex and the subcortical areas that control avoidance behaviours[58], regardless of the pathway the signal travels. This structure is essentially comprised of GABAergic inhibitory striatal projecting neurons (SPNs) (also referred to as medium spiny neurons) as they represent around 95% of the neuronal population in the striatum[61]. These SPNs mostly express dopamine receptors and can be further categorised in two primary subpopulations depending on their phenotype into D_1-receptor-expressing SPNs (D_1R-SPN) or D_2-receptor-expressing SPNs (D_2R-SPN) with each being linked with either the direct or indirect pathway, respectively[62].

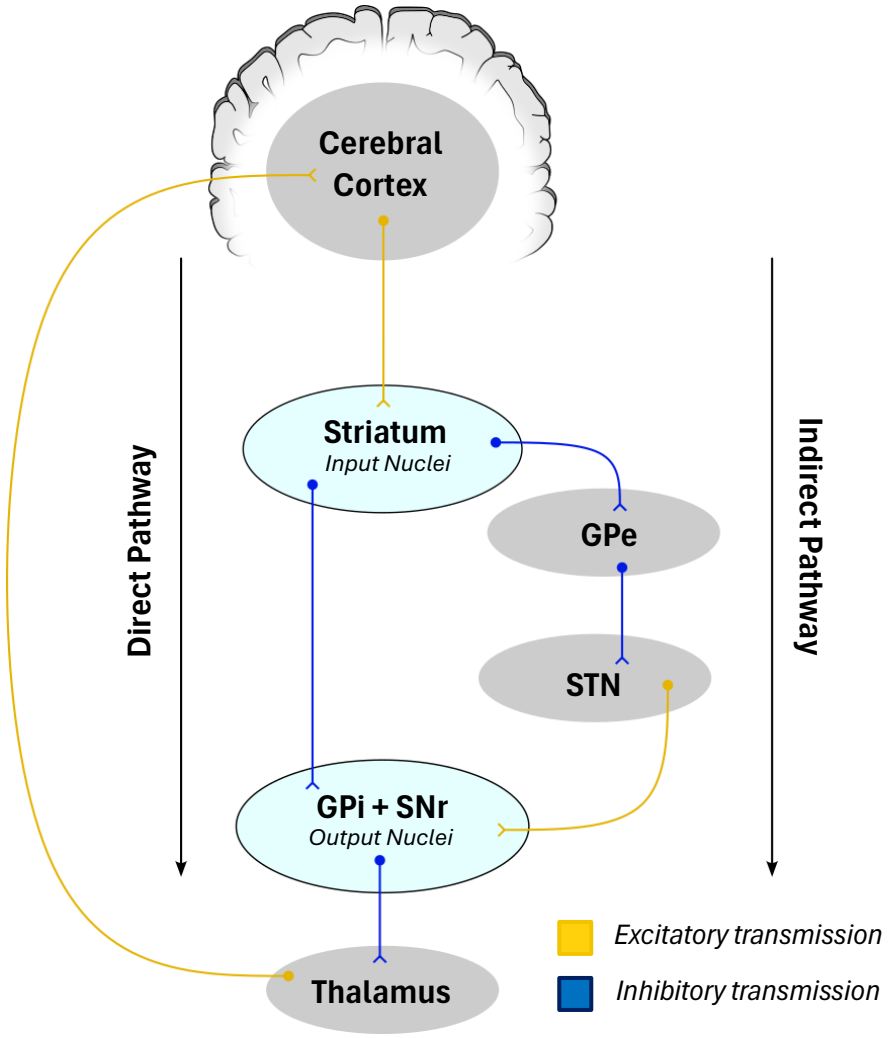


Figure 2 | General schematic of Basal Nuclei direct and indirect pathways. The cerebral cortex sends glutamatergic (excitatory) projections to the striatum. From there, two pathways modulate the output nuclei: the direct pathway (left) projects onto the GPi and SNr with an inhibitory signal, which facilitates movement by disinhibiting the signal relayed to the thalamus; the indirect pathway (right) relays GABAergic signals through the GPe and STN, the latter providing glutamatergic excitation onto the output nuclei, suppressing movement by potentiating the inhibitory synapses from the output nuclei to the thalamus. The thalamus sends excitatory projections back to the cortex, closing the loop and allowing for fine movement regulation.

The striatum has been anatomically organised into dorsal and ventral striatum. However, due to its distinct connectivity, another anatomical division has emerged with a focus on the caudal-most part of the dorsal striatum, the tail of the striatum (TS) in rodents or caudate tail (CDt) in primates[63].

The TS's primary excitatory afferent innervation comes from the sensorimotor, visual, and auditory cortices but it also receives subcortical inputs from regions like the amygdala, as well as thalamic nuclei. TS monoaminergic neuromodulation occurs through either dopaminergic innervation from the SN pars lateralis (SNpL), a connection that has similarly been reported in primates, or, through serotonergic innervation from the dorsal raphe nucleus (DRN)[63]. As for the efferent output signals relayed from the TS to downstream areas, those nervous impulses are sent from the previously mentioned SPN populations with D_1R-SPNs projecting to the GPi and SNr, sending net excitatory output signals through the direct pathway, and D_2R-SPNs projecting to the GPe, sending net inhibitory signals through the indirect pathway[64] (Figure 3).

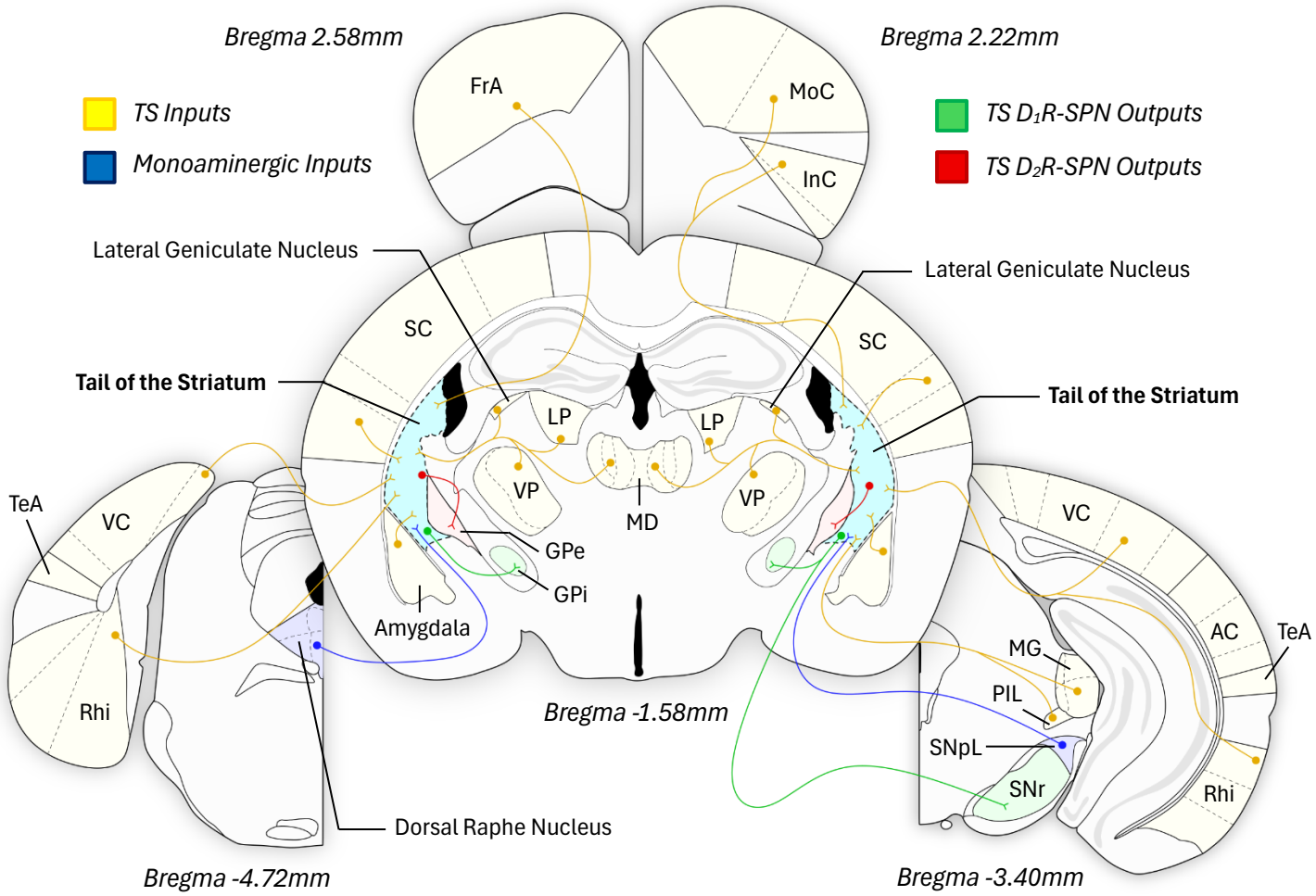


Figure 3 | Schematic summary of the TS's connectivity. Coronal schematics of the mouse brain as a summary of input and output pathways of the TS (cyan). Inputs (yellow) stem from a broad set of sensory and association cortices, as well as subcortical and thalamic nuclei. Monoaminergic inputs (blue) arise from the SNpL for the case of dopamine and the DRN for serotonin. TS outputs are presented in a cell-type dependent segregation with direct-pathway D_1R-SPNs (green) projecting to the GPi and SNr and the indirect-pathway D_2R-SPNs (red) projecting to the GPe. Abbreviations: AC, Auditory Cortex; DRN, Dorsal Raphe Nucleus; FrA, Frontal Association Cortex; GPe, external *Globus Pallidus*; GPi, internal *Globus Pallidus*; InC, Insular Cortex; LP, Lateral Posterior Nuclei; MD, Mediodorsal Nuclei; MG, Medial Geniculate Nucleus; MoC, Motor Cortex; PIL, Posterior Intralaminar Nucleus; Rhi, Rhinal Cortices (ecto-, endo-, peri-); SC, Somatosensory Cortex; SNpL, *Substantia Nigra pars Lateralis*; SNr, *Substantia Nigra pars Reticulata*; TeA, Temporal Association Cortex; VC, Visual Cortex; VP, Ventral Posterior nuclei.

The TS plays key roles in sensory integration, attentional shift, and goal-oriented behaviours, especially when it comes to threat detection, avoidance, and defensive behaviours[65] with some auditory-driven tendencies, as would be expected due to the copious inputs received from the auditory cortex and auditory thalamus, and reported robust responses to sound[66], prompting several studies to designate this region as "the auditory striatum"[67]. On the topic of avoidance behaviours, the functional role of the TS is interlinked with its dopaminergic innervation. In this structure, dopamine dynamics correlate with behavioural responses to the aversive stimuli[65]. The dopamine (DA) neurons that project to the TS stem almost exclusively from the SNpL and, upon optogenetic stimulation, have been shown to promote avoidance behaviours to conditioned aversive stimuli[68]. Highlighting the role of TS dopamine signalling in aversive learning, ablation of TS-projecting dopamine neurons with 6-hydroxydopamine (6-OHDA) reduced avoidance behaviours following the pairing of a stimulus with an aversive outcome[69]. Moreover, these dopaminergic TS-projecting neurons have also been proven to receive direct projections from the auditory association cortex (encompassing the temporal association cortex and the secondary auditory cortex) when compared to other neurons in the SN and synaptic interruption of this circuit decreased formation of auditory threat memories[70] further highlighting SNpL dopaminergic relevance in the establishment of auditory avoidance behaviours.

The downstream effects of dopamine release in the TS in this context seem more cell-type specific as different outcomes arise from the activation of D_1R-SPNs versus D_2R-SPNs. Fiber photometry recordings revealed that avoidance behaviours were associated with elevated D_1R-SPN activity relative to D_2R-SPNs, whereas this pattern reversed when mice overcame the threat[69]. Confirming these correlational findings, cell-type specific ablations using diphtheria toxin subunit A demonstrated that ablation of D_1R-SPNs reduced avoidance behaviours, whereas ablation of D_2R-SPNs impaired the ability to overcome a potential threat[69]. Overall, these results indicate that the D_1R-SPNs in the TS promote threat avoidance, whereas D_2R-SPNs promote the overcoming of the threat, with dopamine levels modulating the balance between them.

1.4 A Dopamine Overview

In the central nervous system, dopamine is a neurotransmitter mainly produced in the ventral tegmental area (VTA), the substantia nigra (SN), and, though comparatively in lower levels, in the tuberal region of the hypothalamus, and projects through 4 major pathways: the mesolimbic pathway (VTA → *Nucleus Accumbens*) where it's related to reward-aversion cognition; the mesocortical pathway (VTA → Prefrontal Cortex), where it's associated with executive functions; the nigrostriatal pathway (SN → Striatum), where it's linked to motor function, reward-aversion cognition and behaviours, as well as associative learning; and the tuberoinfundibular pathway (Hypothalamus → Pituitary Gland) where it's involved in the regulation of prolactin secretion.

1.4.1 Synthesis, transmission, and termination

Molecularly, dopamine is a catecholamine primarily synthesised from the L-tyrosine amino acid. Tyrosine is carried through the bloodstream to the brain where it gets converted into L-DOPA (also known as Levodopa) by the enzyme tyrosine hydroxylase (TH). This first hydroxylation reaction is the rate-limiting step of the dopamine synthesis pathway, and it conditions the amounts of dopamine produced. After this step, L-DOPA is converted into dopamine by a L-amino acid decarboxylase (AADC). The resulting dopamine molecule can further be metabolised in noradrenergic or adrenergic neurons into norepinephrine by the dopamine β-hydroxylase enzyme which, in turn, can result in an epinephrine molecule by introducing a methyl group through the phenylethanolamine N-methyltransferase enzyme (Figure 4).

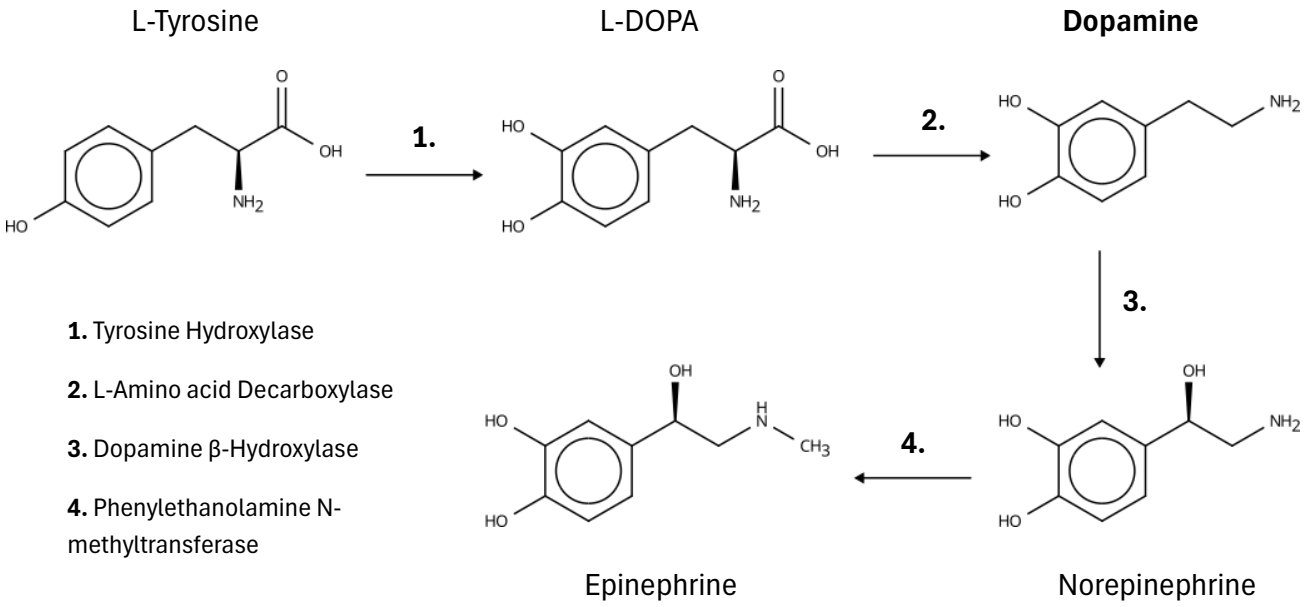


Figure 4 | Dopamine synthesis and metabolism pathways. L-tyrosine is converted to L-DOPA by the TH enzyme. L-DOPA is converted to dopamine by the AADC enzyme. Dopamine can be metabolised into norepinephrine by the DβH enzyme. Norepinephrine is converted to epinephrine by the PNMT enzyme.

Once synthesised, dopamine is released into the synaptic cleft by the presynaptic neuron, acting upon the dopamine receptors in the postsynaptic neuron. Dopamine receptors are metabotropic G-protein coupled receptors and can be divided into two main subclasses, the D_1-like and D_2-like receptors. The D_1-like group encompasses the **D_1** (most expressed in the striatum, the SNr, the *nucleus accumbens*, the hypothalamus, the frontal cortex and the olfactory bulb) and **D_5** (most expressed in the SNc, the hypothalamus, the striatum, the cerebral cortex, the *nucleus accumbens*, and the olfactory tubercule) receptors which couple to G_s leading to an increase in intracellular cyclic AMP (cAMP) and, consequently, lead to a downstream excitatory effect. Conversely, the D_2-like group encompasses the **D_2** (most expressed in the striatum, the *nucleus accumbens*, the olfactory tubercule, the prefrontal cortex, the amygdala, the VTA, the hippocampus, the hypothalamus, and the SNc), **D_3** (most expressed in the striatum, the *nucleus accumbens*, the SNc, and the VTA) and **D_4** (most expressed in the retina, but also found in the hypothalamus, the prefrontal cortex, the amygdala, and the hippocampus) receptors which couple to $G_{i/o}$ proteins, reducing intracellular levels of cAMP and causing a downstream inhibitory effect. Importantly, D_2 and D_3 receptors can also be located at the axon terminal of the presynaptic neuron, playing an auto-inhibitory role that helps regulate dopamine activity.

Following an elicited response, dopamine becomes unbound from the respective receptor and proper clearance mechanisms ensue to prevent a rebinding and consequent overactivation of the postsynaptic neuron. While dopamine can be metabolised intracellularly by the monoamine oxidase (MAO) or catechol-O-methyltransferase (COMT) enzymes, the primary mechanism for termination of dopamine action is through reuptake by specific dopamine transporters (DAT) which are mainly located in the membrane of the presynaptic neuron.

1.4.2 Subregional dopamine signalling in the TS

Striatal dopaminergic abnormalities are well associated with neurological disorders like Parkinson's or Huntington's disease. However, as previously mentioned, the striatum is a heterogeneous region divided into different domains with different connectivity and functions. In rodents, the TS specifically, is further divided into subregions following D_1R- and D_2R-SPNs' distribution along the dorsal, medial, intermediate, and lateral regions of the TS. While the lateral and dorsal tail subdivisions have been documented as presenting a somewhat homogeneous distribution of SPNs subpopulations, the medial subdivision presents a predominant expression of D_1R-SPNs, contrasting the intermediate subdivision with its prevailing D_2R-SPNs, establishing a type of segregation that appears unique to the TS.

Dopaminergic innervation in the TS has been shown to be reduced when compared to other striatal regions. In rat brain slices, while the main identified dopamine clearance mechanism, independently of TS division, was reuptake by DAT, fast scan cyclic voltammetry (FSCV) and pharmacological tests have revealed different regional profiles of dopaminergic release with the lateral and medial subdivisions showing increased levels. Notably, the characteristically TH-poor intermediate subdivision displayed the lowest amplitude of evoked dopamine release, as well as a particularly slowed dopamine clearance rate when compared to the other subdivisions which has been hypothesised to result from disparities in dopaminergic availability and innervation. However, similar results regarding dopamine release were observed in the dorsal subregion of the TS which has a TH level of expression akin to what was found in the remaining division.

These results highlight each subdivision's unique dopaminergic profile in terms of balancing dopamine release and clearance and yet, despite such reports, the downstream implications of these findings at a sensorial level remain largely unexplored.

1.4.3 The dopamine system in ASD

ASD have been hypothesised to be related to dopamine dysfunctions, with different brain-region specific disruptions in dopaminergic transmission in the midbrain being associated with the social deficits and stereotyped behaviours core to the disorder.

Studies conducted in individuals with ASD have revealed alterations in the mesocortical and mesolimbic pathways with reduced neural responses surrounding the *nucleus accumbens* as well as lower levels of dopamine release in the prefrontal cortex in PET scans[1], supporting the idea that a mesocorticolimbic circuit-associated malfunction could lead to a lower perceived rewarding sensation in social connections, causing a decrease in social drive and, consequently, social skill improvement. This cycle, is fundamentally summarised in the social motivation theory of ASD which proposes that a lower social drive leads to impairments in social skill or cognition, resulting in the social deficits reported as a characteristic of autism. Research done in mice have supported the importance of this pathway in socialising behaviours by optogenetic modulation of dopaminergic neurons in the VTA, with this area's activation resulting in an increase of social behaviours in mice, contrasting with the results of VTA inactivation.

Regarding the nigrostriatal pathway, that circuit has been proposed as being linked to the stereotyped behaviours reported in ASD. Essentially, given this pathway's role in mediating goal-oriented behaviours, impairments associated with it may lead a person to a cycle of repetition as associated with RRBs, which is supported by findings of mutations in genes encoding for DAT and DA receptors being linked with such behaviours. Particularly, in mice, dysfunctions to the nigrostriatal pathway like D_1R-SPN activation by suppressed

expression of DAT in the SN have emerged as autistic-like behavioural phenotypes, while the administration of D_1R antagonists lead to a reduction in such results.

1.5 The end goal

Imbalances in the dopaminergic circuitry have been reported in ASD for a long time[71] but their part in sound processing and potential pathophysiological relation to the avoidance behaviours remain unexplored. In this study we aim to understand how the dopaminergic system is altered in the SNpL-TS circuitry and its implications in auditory avoidance.

1.5.1 Animal model of ASD: *Shank3* KO mice

To properly study a given feature of ASD it's necessary to employ the right animal model. As previously mentioned, there is no known single aetiological factor responsible for ASD and many models have surfaced recreating one or more of the factors found to be linked with this disorder. Of the environmentally dependent models, foetal exposure to valproic acid has been one of the most thoroughly described in rodents, showcasing a plethora of ASD-like traits such as reduced sociability, weakened sensory gating observed as reduced PPI, anxiety-like behaviours, and increased repetitive behaviours like self-grooming and nest shredding[72]. While non-genetic models are valuable for studying developmental mechanisms as they introduce the possibility for time-frame-specific administration, genetic models provide robust construct validity, and often facilitate more consistent cross-study reproducibility[73].

As described in Section 1.1, among the numerous risk genes linked to ASD, *SHANK3* represents one of the most consistently implicated genes across large-scale genomic analyses of ASD. SH3 and multiple ankyrin repeat domains (SHANK) proteins are a family of key structural proteins in the postsynaptic density present in neuronal synaptic scaffolding systems of excitatory synapses encoded by three different genes (*SHANK1*, *SHANK2*, and *SHANK3*) with the *SHANK3* being the best studied of them[74]. Pathologically, this gene gained relevance for its associated findings in the Phelan-McDermid Syndrome (PMS), a genetic neurodevelopmental disorder presenting with developmental delay, decreased muscle tone, and ASD-like features such as difficulties social interactions and repetitive behaviours to the point that up to 80% of the population affected by it have an overlapping ASD diagnosis[75,76]. It's caused by a genetic mutation in the human chromosome 22 at the q13.3 position resulting in the loss of function of the SHANK3 protein[77] and, when recreated in mice leads to key ASD behavioural phenotypes, namely repetitive behaviours in the form of compulsive self-grooming, reduced sociability and reciprocal interaction[78], anxiety-like behaviours, and sensory hyperreactivity both in the tactile[79] and, the auditory domain, showcasing possible auditory avoidance behaviours[80].

For this work, the mouse model used recreates a mutation reported in autistic individuals with the insertion of a guanine in place of the 3680th nucleotide in the *Shank3* gene, ceasing protein expression by causing a frameshift mutation and leading to an early stop codon[81]. This specific transgenic mouse line is often found in literature as *Shank3*-InsG3680$^{(+/+)}$ but, for this dissertation it will be referred to as *Shank3* KO.

1.5.2 Hypothesis and Objectives

Autistic people recurringly report decreased sound tolerance as a hindrance to day-to-day life, particularly in work and social settings. This reflects a mismatch between what neurotypical individuals would perceive as a harmless auditory scenario and what is experienced as aversive by autistic individuals, often resulting in self-withdrawal and avoidance behaviours from individuals with ASD, contributing to feelings of loneliness and decreasing overall quality of life. No mechanism has yet been objectively identified to be responsible for this heightened avoidance phenotype in autistic people, hampering the development of therapies.

Dopaminergic dysregulations have been described as a hallmark of autism[71] and, dopaminergic neurons projecting from the SNpL to the TS have been consistently shown to modulate avoidance behaviours in WT mice. Building on this, the present work aims to determine whether molecular mechanisms in the dopaminergic SNpL-TS circuitry are altered in a *Shank3* KO compared to WT mice. To achieve this aim, a custom-designed auditory avoidance behavioural test developed by the laboratory will first be used to assess auditory avoidance behaviours in this autism mouse model. Subsequently, the dopaminergic system will be characterised anatomically and molecularly, using techniques such as immunohistochemistry and western blotting. Finally, dopaminergic receptors will be pharmacologically modulated during the auditory avoidance test to evaluate their contribution to the observed avoidance phenotype.

Materials and Methods

- *ANIMAL MODEL*
- *GENOTYPING*
- *STEREOTAXIC INJECTIONS*
- *BEHAVIOURAL TESTS*
- *WESTERN BLOTS*
- *IMMUNOHISTOCHEMISTRY (IHC)*
- *IMAGE ACQUISITION AND ANALYSIS*
- *STATISTICAL ANALYSIS*

2 | MATERIALS AND METHODS

2.1 Animal model

The animal models used in this work were C57/BL6 mice (males and females, 8-12 weeks old) and were separated into either WT or *Shank3*-InsG3680$^{+/+}$ by genotype. Animals were housed under controlled conditions with an automatic 12-hour light/12-hour dark light cycle, a set room temperature at 23 ± 1ºC, room humidity between 50-65% and available food and water *ad libitum*. All animal procedures were conducted in accordance with Portuguese government's National Authority for Animal Health (DGAV) licensing and regulations, as well as the guidelines set forth by the institution's Animal Welfare and Ethics Body on the use of animals for research purposes.

2.2 Genotyping

Animal genotypes were confirmed through Polymerase Chain Reaction (PCR) analyses of either tail or ear samples collected from postnatal day 10 (P10) pups and stored at -20ºC. To that effect, the harvested tissue was incubated for 30 minutes (for tail samples) or 1 hour (for ear samples) at 95ºC in an alkaline solution (25mM NaOH, 0.2mM EDTA, pH=12.0) which was then neutralized with the addition of an equal volume of acidic solution (40mM Tris-HCl, pH=5.0) for DNA extraction and stored at 4ºC until used for PCR.

For PCR amplification, 1µl of the DNA template was added to 9µl of master mix (5µl of MyTaq Mix (Bioline #BIO-25042), 3.2µl of Milli-Q water, and 0.4µl of 10mM solutions of forward and reverse primers (Table 1)) and subsequently subjected to PCR cycling conditions as described below (Table 1). To the resulting solution was then added 2µl of Bromophenol Blue and the mixture was loaded onto a 1.5% agarose gel (TAE). The gel was run at 120V, and amplification products were observed using the Chemidoc™ MP imaging system (Bio-Rad). The resulting bands were analysed by comparing the obtained bands to control ones from animals with known genotypes (WT and heterozygous (*Shank3*-InsG3680$^{+/-}$)).

Table 1 | Primer sequences and PCR conditions for genotyping of *Shank3*-InsG3680$^{+/+}$

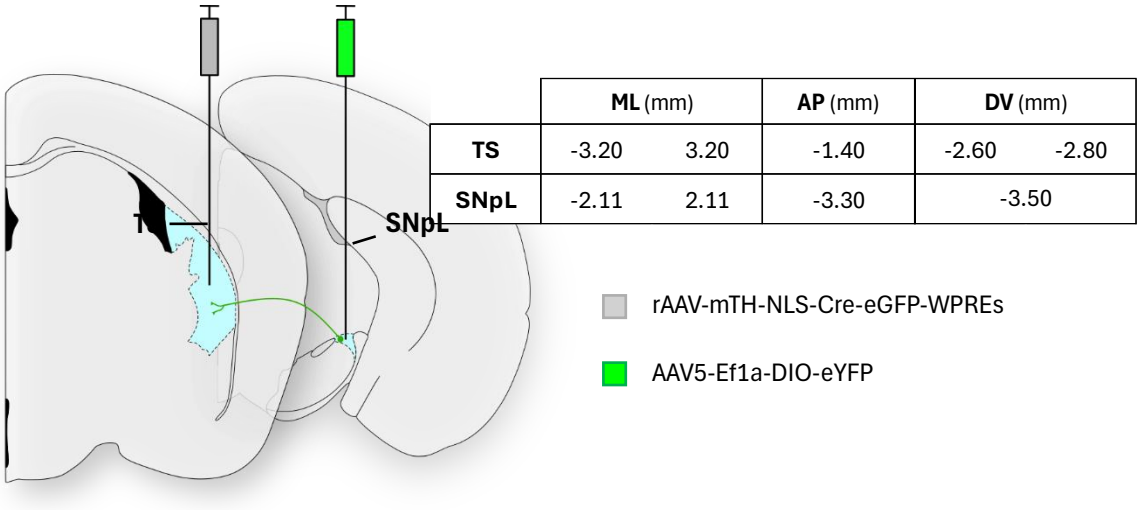
Genotype	Primer	Primer Sequence (5' to 3')	PCR Conditions
Shank3	Forward	5'- ACC CCT CTT TGT GGA TGT GCA AAC CCG AGA CTC-3'	95ºC – 4' 95ºC – 30" 58ºC – 20" 72ºC – 30" (30x) 68ºC – 10' 4ºC – ∞
	Reverse	5'- GTT CAC AGC GAA TAC CAG CTC TGG CTC CTC CTC-3'	

2.3 Stereotaxic Injections

Before stereotaxic surgery, mice were induced into anaesthesia with sevoflurane (Abbvie, FR-ABBV-240124) dissolved in gaseous O_2 at a flow rate of 5 L/min in an induction chamber. Upon successful induction indicated by an observable decrease in breathing and heart rate, and lack of paw withdrawal reflex, the animal was placed on the stereotaxic frame (World Precision Instruments) with the snout inside a custom mask that doubled as an incisor bar and directed sevoflurane/O_2 gas flow, which had a rate reduction to 2-3 L/min for anaesthesia maintenance, being adjusted when necessary. The eyes were kept lubricated by the application of Vaseline with a cotton bud to avoid corneal damage and the cranium was secured in place by the insertion and adjustment of ear bars. Mice were injected subcutaneously with a 0.9% NaCl saline solution as well as with a buprenorphine (Bupaq) solution diluted in 0.9% NaCl to a 3µg/mL final concentration.

Thus, the animal's scalp was cut open with a micro-dissection scissors and with the skull exposed, the head was aligned symmetrically in all three dimensions with proper balancing done from Bregma. From there, four holes were bored with a drill at the coordinates needed to target bilaterally the TS (AP: -1.40mm; ML: ±3.20mm) and the SNpL (ML: ±2.11mm; AP: -3.30mm) enough to perforate the cranium and meningeal layers.

For the injection, glass capillaries previously pulled in the lab (Drummond Scientific, 08 3203 G/X) were filled with mineral oil (Sigma, M8410-100ML) and, after ensuring the lack of any air bubbles, introduced into its respective Nanoject II (Drummond Scientific) slot where they were finally filled with the viral solutions to be injected (Figure 5).



	ML (mm)		**AP** (mm)	**DV** (mm)	
TS	-3.20	3.20	-1.40	-2.60	-2.80
SNpL	-2.11	2.11	-3.30	-3.50	

Figure 5 | Graphic summary of viruses and coordinates considered for stereotaxic surgery to target the TS and the SNpL. Schematic injection layout in coronal slices of a mouse brain with the TS and SNpL regions highlighted.

After readjusting the stereotaxic arm's ML and AP coordinates from Bregma to account for the capillary, its tip was slowly lowered to the respective DV coordinates (Figure 5) and the viral solutions were dispensed at an injection rate of 23nL/s, with a total volume of 56nL injected. The capillary stood at the injection site for 5 minutes after the injection to avoid backflow on its retreating path.

Upon completion, the scalp was sutured along the initial incision's length, and the animal was removed from the stereotax, later being sacrificed 5 weeks after surgery for histological processing and analysis.

2.4 Behavioural tests

All behavioural tests were conducted inside a sound- and light-proof cage. Infrared light was used to visualise and record the mice. Video footage was recorded at 30 fps from a top-down point of view using an infrared camera (FLIR, FL3-U3-13Y3M-C).

When intraperitoneal injections were to be applied, mice were divided into 2 groups and administered with either the drug of study, Pramipexole (Alfagene) at a concentration of 0.3mg per kg of the animal's body weight or 0.9% NaCl saline solution, for the case of the control group animals, 1h before the behavioural test took place.

2.4.1 Auditory Looming Paradigm

To investigate auditory avoidance behaviours, an auditory looming paradigm developed by the laboratory was employed. The test was performed in dark conditions in a custom-made square arena (40 × 40 cm) with opaque white walls, and individual animals were tracked in real time with a Bonsai-coded algorithm (Reis et al., unpublished). In a corner inside of the arena was placed a piece of the animal's home cage nest. A 3-minute baseline period was first recorded to allow the animal to acclimate to the arena, followed by a 10-minute testing period in which a crescendo white noise sound played from an electrostatic speaker (ES1, Tucker-Davis Technologies) automatically triggered by the detection of the animal's entry into a designated region of interest (ROI) repeating for as long as the mouse was inside and ceasing upon its exit.

2.4.2 Homecage test

Mice were left inside their home cages with fellow cage mates for 10 minutes with no auditory stimuli being played and their activity was recorded and captured by the infrared camera.

2.4.3 Behavioural Analysis

Mice behavioural performance in the auditory looming task was analysed digitally by a custom-made MATLAB script coded by the laboratory (Reis et al., unpublished) in three parameters: the number of times the animal stepped inside the ROI, the amount of time the animal spent in its nest, and the total travelled distance within the arena.

For the home-cage evaluation, the time each animal spent in locomotion within its home-cage was manually assessed and further analysed.

2.5 Western Blots

2.5.1 Protein extraction and quantification

Mice were anaesthetised with an intraperitoneal injection of a tribromoethanol solution diluted in PBS to a concentration of 20 mg/mL and transcardiacally perfused with artificial cerebrospinal fluid (aCSF) solution (119mM NaCl, 2.5mM KCl, 1.2mM NaH_2PO_4, 24mM $NaHCO_3$, 12.5mM glucose, 2mM $MgSO_4 \cdot 7H_2O$, 2mM $CaCl2 \cdot 2H_2O$; pH=7.3). The brains were removed, sliced with a vibratome (Leica VT1000 S, 11483) at a thickness of 500µm in a carbogen-aerated aCSF solution, and macrodissected to isolate the TS and the SN. The collected brain regions were then flash frozen in liquid nitrogen and stored at -80ºC until further processing.

For protein extraction, each sample started by being resuspended and homogenised through up and down pipetting in radioimmunoprecipitation assay (RIPA) buffer (150mM NaCl, 0.1% Sodium Dodecyl Sulphate (SDS), 50mM Tris-Base, 1% Triton X-100, 0.5% deoxycholate) supplemented with protease inhibitors (Roche, 11873580001) and phosphatase inhibitors (Roche, 4906845001) while being kept in ice whenever possible, followed by sonication for 15 minutes at the highest intensity. The resulting solution was centrifuged at 20000 x g and 4ºC for 15 minutes and the supernatant was collected.

Protein quantification was done with a BCA assay kit (Thermo Scientific, 23225) and spectrophotometry. Bovine serum albumin (BSA) solutions were prepared diluted in water at different concentrations and, as well as with the extracted protein solutions from the brain tissues, incubated at 37ºC for 30 minutes with BCA working solution (Reagent A to Reagent B ratio of 50:1). The absorbances were then measured at 562nm and the BSA values were used to set up a standard curve from which sample protein concentration was calculated with the Beer-Lambert law.

2.5.2 SDS-PAGE

Polyacrylamide gradient gels were cast with a 5% acrylamide portion for protein stacking (Bis-acrylamide (Bio-Rad, 1610146), 0.5M Tris-base-HCl (pH=6.8), SDS 10%, ammonium persulfate (APS) 10%, and tetramethyl ethylenediamine (TEMED) 1%) and a 10% acrylamide portion for protein resolving (Bis-acrylamide (Bio-Rad, 1610146), 0.5M Tris-base-HCl (pH=8.8), SDS 10%, ammonium persulfate (APS) 10%, and tetramethyl ethylenediamine (TEMED) 1%).

Fifteen µg of mouse brain protein were mixed in with β-mercaptoethanol-supplemented Laemmli sample buffer (Bio-Rad, 1610737EDU), incubated at 70ºC for 10 minutes, and loaded in triplicates to the previously cast gels now submerged in running buffer (25mM Tris-Base, 192mM Glycine, 0.1% SDS) and so was the molecular weight ladder (Thermo Scientific, 26634). The gel was run at 70V to allow the sample solutions to align at the interface between the stacking and resolving gels after which, it was run at 120V until the tracking dye left the gel.

Proteins were wet transferred from the polyacrylamide gel to a nitrocellulose membrane (Bio-Rad, 1620112) in cold transfer buffer (25mM Tris-Base, 192mM Glycine, 20% methanol) at 90V for 1h.

2.5.3 Immunoblotting

Upon successful transfer confirmation with Ponceau S (Sigma-Aldrich, P3504-10G) staining, the protein-laden membrane was blocked for 1h at room temperature (RT) in blocking solution (5% milk in Tris Buffered Saline (192mM Tris-HCl, 25mM Tris-Base, and 0.1% NaCl) with 0.05% Tween-20 (TBS-T)) on an orbital shaker. The membranes were then incubated overnight at 4ºC with the appropriate primary antibodies in blocking solution (Table 2).

The following day, the membranes were washed 3 times for 10 minutes at a time with TBS-T on an orbital shaker, subsequently being incubated at RT for 90 minutes with the corresponding secondary antibodies in blocking solution (Table 2) and washed a final 3 times in TBS-T as previously described.

The secondary antibody signal was revealed using an enhanced chemiluminescent (ECL) horseradish peroxidase (HRP) substrate (Thermo-Scientific, 34580) applied directly to the membrane for 3 minutes and detected with the Chemidoc™ MP imaging system (Bio-Rad). The captured image was analysed with Image Lab Software v6.1 (Bio-Rad) and the relative protein levels were measured and normalised for the respective β-actin band intensity values.

Table 2 | Primary and secondary antibodies used for immunoblotting

Primary Antibody	Dilution	Supplier	Secondary Antibody	Dilution	Supplier
α-Tyrosine Hydroxylase (Rabbit)	1:2000	Synaptic Systems, 213 102	**HRP-conjugated α-Rabbit IgG (Goat)**	1:10000	Jackson ImmunoResearch, 111-035-003
α-Dopamine Transporter (Rabbit)	1:2000	GeneTex, GTX133152			
α-β-actin (Mouse)	1:10000	Sigma-Aldrich, A5441-100UL	**HRP-conjugated α-Mouse IgG (Goat)**	1:10000	Jackson ImmunoResearch, 115-035-003

2.6 Immunohistochemistry (IHC)

Mice brains were removed as previously described in the Western blot 2.5.1 section differing only in the solution used for the transcardiac perfusion. In place of aCSF, mice were pumped with 1X PBS, followed by 4% paraformaldehyde (PFA). After being collected, the brains were left in 4% PFA overnight which was then replaced by 1X PBS until further use.

For sectioning, the brains were left submerged in a 30% sucrose solution for at least 48h before being embedded in OCT compound (Tissue-Tek, 4583), sliced with a cryostat (Medite, M650) at a thickness of 50µm and collected in multi-well plates filled with 1X PBS for free-floating IHC staining.

After washing the slices once with 1X PBS to remove excess OCT compound, the sections were blocked at RT for 1h in blocking buffer solution (10% Goat Serum and 0.3% TritonX in 1X PBS) on an orbital shaker. Once blocked, slices were incubated at RT for 30 minutes with the primary antibodies (Rabbit-α-Tyrosine Hydroxylase, 1:1000 (Synaptic Systems, 213 102), and Mouse-α-NeuN, 1:500 (Sigma-Aldrich, MAB377)) diluted in blocking buffer and then left agitating overnight at 4ºC. The next day, the slices were washed 3 times with 1X PBS with 0.3% TritonX for 10 minutes at a time on an orbital shaker at RT and incubated with the secondary antibodies (647-Goat-α-Rabbit IgG, 1:1000 (Invitrogen, A21245), and 488-Goat-α-Mouse IgG, 1:1000 (Invitrogen, A11029)) diluted in blocking buffer for 2h at RT protected from light. Following the secondary antibody step slices were incubated with DAPI (1:1000, (Panreac Applichem, A1001)) diluted in 1X PBS for 10 minutes and washed one final time with 1X PBS. TS- and SNpL-containing sections

were mounted onto glass slides and loaded with Immu-Mount™ (Epredia, 9990402) as mounting media for future image acquisition.

2.7 Image acquisition and analysis

Fluorescent images were obtained with the Zeiss Axio Imager Z1 optical microscope at a 20x lens magnification and put together with the Zeiss Tiles function.

Image analysis was done with the Fiji (ImageJ) software. For signal intensity analysis, the relevant areas for each slice were traced and the mean grey values obtained. Specific-cell-body counting was done manually and normalised for total number of cells for that respective area. All measurements were done in at least 3 different slices per animal with the final value considered for analysis being the average of all.

2.8 Statistical Analysis

All statistical analyses and graphed data were obtained with GraphPad Prism 8 software. Normality was assessed with the Shapiro-Wilk test due to reduced sample sizes, and outliers were identified and removed with Grubbs' test at a 0.2 significance level.

When comparing two independent sets of data, analyses were carried out with two-tailed unpaired t-test with Welch's correction when normality was verified, or with Mann-Whitney test if it wasn't. Statistical significance was considered when the reported p-value ≤ 0.05.

Results

- *THE SNpL-STRIATAL CIRCUIT IS CONFIRMED IN MICE*
- *SHANK3 KO MICE SHOW INCREASED AVOIDANCE BEHAVIOURS TO AUDITORY LOOMING STIMULI*
- *TYROSINE HYDROXYLASE LEVELS SEEM UNALTERED BETWEEN GENOTYPES*
- *D_1Rs MAY BE LESS EXPRESSED IN NEURONS OF SHANK3 KO MICE THAN IN WT MICE*
- *ADMINISTRATION OF D_2R AGONISTS LOWERS OVERALL MOVEMENT*

3 | RESULTS

3.1 The SNpL-Striatal circuit is confirmed in mice

In order to confirm the anatomical connection between the TS and the SNpL and verify the reported presence of nervous inputs from the latter to the former, a Cre-dependent virus coding for eGFP (AAV5-Ef1a-DIO-eYFP) was bilaterally injected into the SNpL of a mouse brain through stereotaxic surgery while a retrograde virus coding for Cre recombinase (rAAV-mTH-NLS-Cre-eGFP-WPREs) was bilaterally injected into the TS of a mouse brain within the same surgical procedure (Figure 6a.), which should, theoretically, lead to an expression of eGFP solely in TS-projecting neurons stemming from the SNpL.

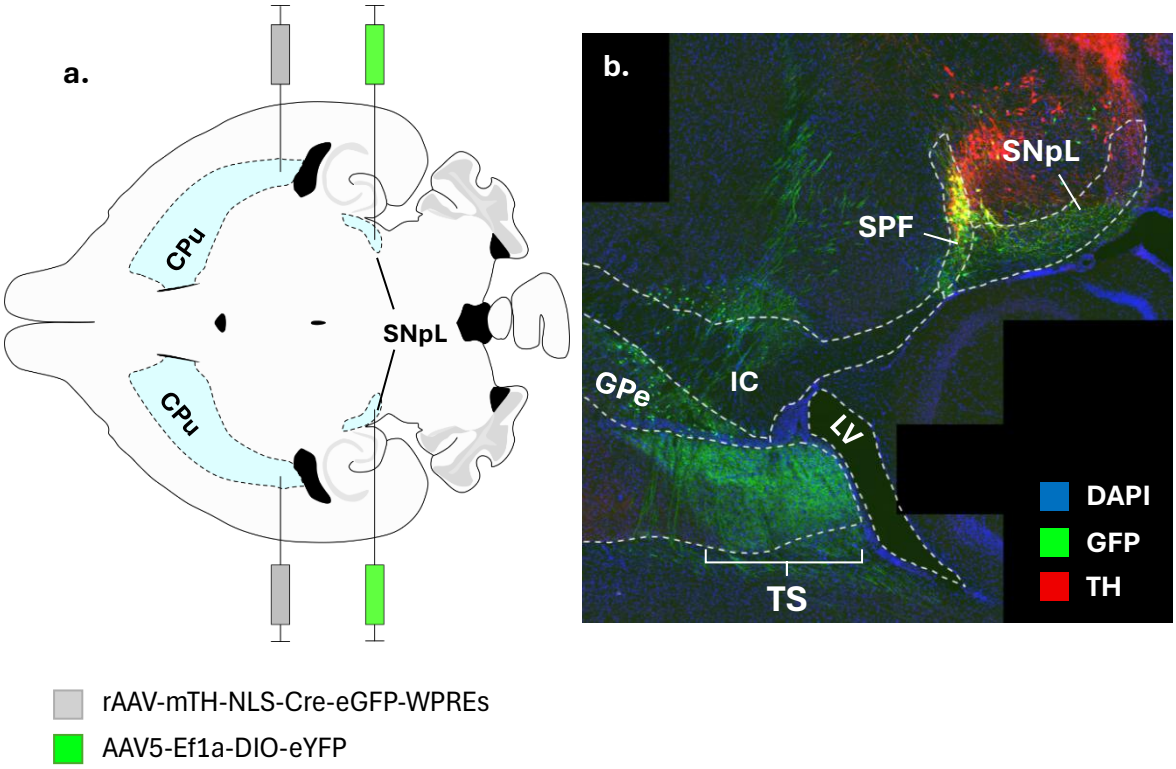


Figure 6 | SNpL neurons show an established projection to the TS. a. Stereotaxic bilateral injection of retrograde rAAV-Cre virus into TS and AAV5-DIO-eGFP into SNpL. **b.** Representative immunofluorescent image of a horizontal brain section of a mouse brain with eGFP in green and TH-stained cells in red. Abbreviations: CPu, Caudate *Putamen*; GPe, external *Globus Pallidus*; IC, Internal Capsule; LV, Lateral Ventricle; SNpL, *Substantia Nigra pars Lateralis*; SPF, Subparafascicular thalamic nucleus

While that expression is, in fact, present, thus showcasing the preservation of a SNpL-Striatal circuit (Figure 6b.), eGFP signal can also be seen in other brain regions that have also been shown to have Striatum-projecting neurons like the GP or the SPF, possibly due to tracer diffusion on the descending path of the glass micropipette to neighbouring structures before reaching the target area at the SNpL. Nevertheless, the presence of said signal confirms the existence of the sought-after circuit in the mouse brain and the focused location of eGFP signal at the caudal-most part of the striatum when compared to the rest

of the CPu area, indicates, at least qualitatively, that these projections are mostly aiming for the TS.

Furthermore, to confirm that the projections seen were effectively dopaminergic, the slices were further stained with a TH antibody meant to confirm the viral specificity for dopaminergic neurons. However, the presence of GFP-only signal (Figure 6b. (green)) separate from the TH-stained signal (Figure 6b. (red)) shows that despite the association of the GFP-coding sequence with a mouse TH promoter, other non-dopaminergic TS-projecting neurons also incorporated the virus indicating a lack of cell-type specificity.

3.2 *Shank3* KO mice show increased avoidance behaviours to auditory looming stimuli

With the circuit's presence confirmed in the mouse brain, the next step was to validate the presence of the ASD-like behavioural phenotypes most relevant to the study in the animal model used, namely the increase in auditory avoidance behaviours. For that, WT and *Shank3* KO mice were subjected to an auditory looming behavioural test (Figure 7a.). Three main parameters were evaluated: the number of times the animal entered the ROI, the time it spent in its nest, and the travelled distance within the arena, allowing the evaluation of avoidance towards a sudden-sound-emitting area, anxiety behaviour, and mobility, respectively.

Throughout the entirety of the test, *Shank3* KO mice consistently enter the ROI less than their WT counterparts (Figure 7b.) while spending similar amounts of time in their nests during both trial periods (Figure 7c.). When anxious, mice often retreat to a corner during open arena behavioural tests, and despite *Shank3* KO mice having been shown to display increased levels of anxiety, the similarity in the time they spent in their nests compared to the time measured in the WT group indicates that the differences in avoidance of the ROI were likely not due to anxiety levels.

As for the evaluation of the distance travelled within the arena, much like the previous parameter, no significant changes arise between KO and WT mice (Figure 7d.) and although *Shank3* KO mice have been reported to showcase lower locomotor activity before, these results allow us to rule out the noted differences in the number of entries in the ROI as being attributable to any locomotive impairments.

Considering the fact that both the time in nest and travelled distance aspects remain statistically indifferent between either group of mice, the lower number of entries in the ROI can likely be ascribed to an increase in avoidance behaviours, thus validating the animal model used as presenting auditory avoidance traits.

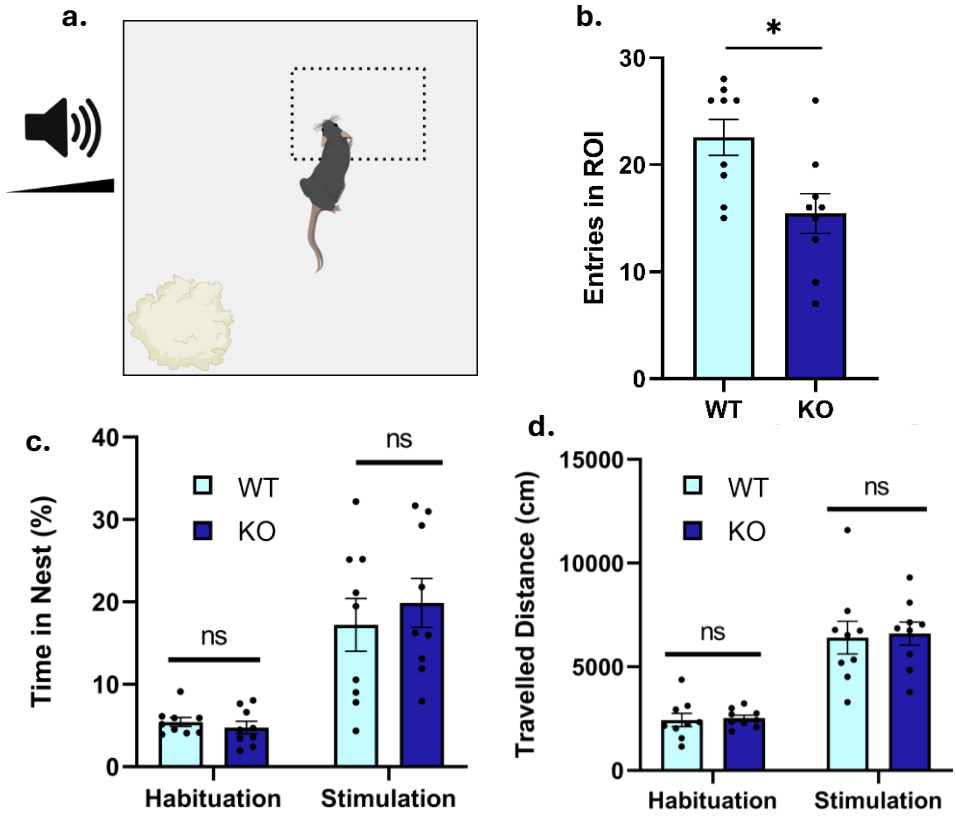


Figure 7 | *Shank3* KO mice enter the auditory looming region less often than WT mice while showcasing negligible differences in the time spent in their nests and travelled distance. a. Diagram of Auditory Looming paradigm: Individual mice are placed in an open arena with a small piece of their nest in the corner (bottom left). After a habituation period of 3 minutes, a 10-minute stimulation period ensues in which a crescendo auditory stimulus starts playing upon the animal's entrance in a designated region of interest (ROI) (dotted rectangle) **b.** Number of times each WT and KO mouse entered the ROI during their trial of auditory looming behavioural test. **c.** Percentage of time each WT and KO mouse spent in their nest during each period of their trial of auditory looming behavioural test. **d.** Distance travelled within the arena by each WT and KO mouse during each period of their trial of auditory looming behavioural test. Values presented as mean ± SEM. ns – no significant difference. *p < 0.05. *(WT: n = 9 mice; KO: n = 9 mice)*.

3.3 Tyrosine Hydroxylase levels seem unaltered between genotypes

In order to assess the hypothesis of altered SNpL->TS dopaminergic pathway in *Shank3* KO mice, a few strategies were employed. A neurotransmitter must meet a few requirements to be considered so, two of which being that it must be synthesised and stored in the presynaptic neuron, and that it must be released by the presynaptic neuron's axon terminal upon stimulation. Looking to these two endpoints, the attention was shifted towards the biochemical pathway of synthesis of dopamine, specifically to the rate limiting step in which tyrosine is converted to L-DOPA by tyrosine hydroxylase (TH) to gauge discrepancies between the WT and *Shank3* KO mice at a production level of dopamine within the TS and SNpL brain regions. The expression levels were evaluated through immunohistochemistry with no statistical analysis done given the small sample size for the WT group, but the levels were later assessed through western blotting.

For the SNpL, being a dopamine-producing region, the immunofluorescent analysis was done by counting the number of cell bodies stained for TH, divided by the total amount of nuclei stained with DAPI for that area (Figure 8a.). Each data point represents one animal and is the average of 3 different slices per animal (Figure 8b.).

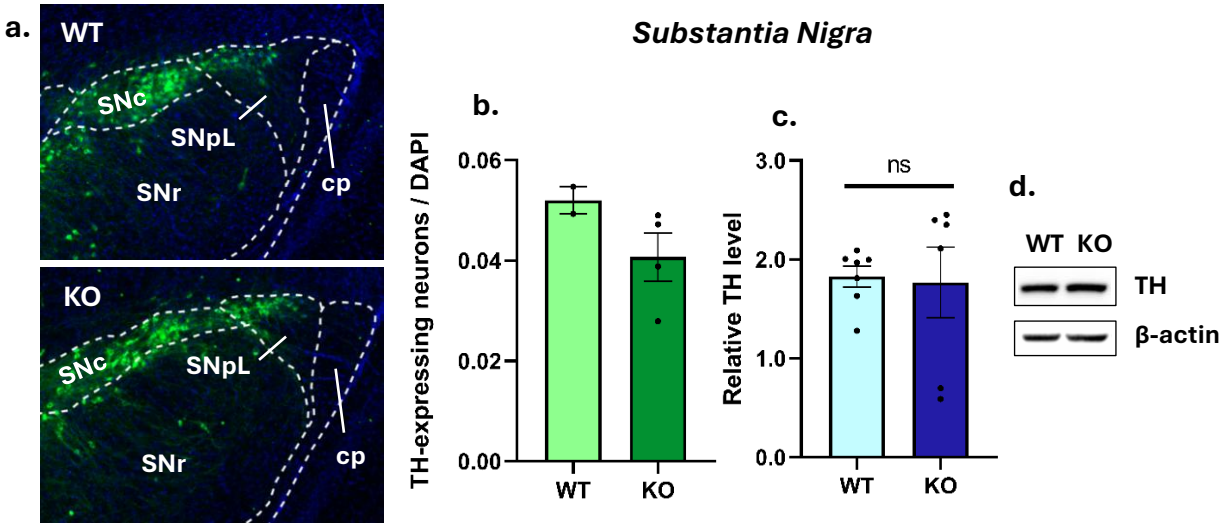


Figure 8 | Immunohistochemical staining of TH in the SN suggests slightly lower levels in *Shank3* KO mice but western blot data shows no differences. a. Representative immunofluorescent images from coronal brain sections of WT (above) and KO (below) mice staining nuclei in blue and TH in green in the SN with 20x objective lens. **b.** Number of TH-expressing cell bodies normalised for total number of DAPI nuclei in SNpL. *(WT: n = 2 mice; KO: n = 4 mice)* **c and d.** Western Blot results. Representative Western Blot of TH and β-actin bands in WT (left) and KO (right) brain tissue from the SN (**d.**) and quantification of TH signal normalised for β-actin (**c.**). *(WT: n = 7 mice; KO: n = 6 mice)*. Values presented as mean ± SEM. ns – no significant difference. Abbreviations: cp, cerebral peduncle; SNc, *Substantia Nigra pars Compacta*; SNpL, *Substantia Nigra pars Lateralis*; SNr, *Substantia Nigra pars Reticulata*.

The resulting data appears to show a slight decrease in TH-expressing neurons in the KO group when compared to the WT mice, which could suggest a lower number of dopaminergic neurons (TS-projecting or not) in the SNpL. However, western blot results obtained from samples of the same brain region, reveal no statistically significant differences in TH levels between groups (Figure 8c. and d.)

As for the TS, the analysis for the immunofluorescent results was carried out differently since this region doesn't have TH-expressing cell bodies. What it does contain, however, are the axons of dopamine-producing neurons that go through it, which can instead be evaluated by tracing the area of the TS (Figure 9a.) and measuring the mean signal intensity in 3 different slices per animal and then averaging those values (Figure 9b.).

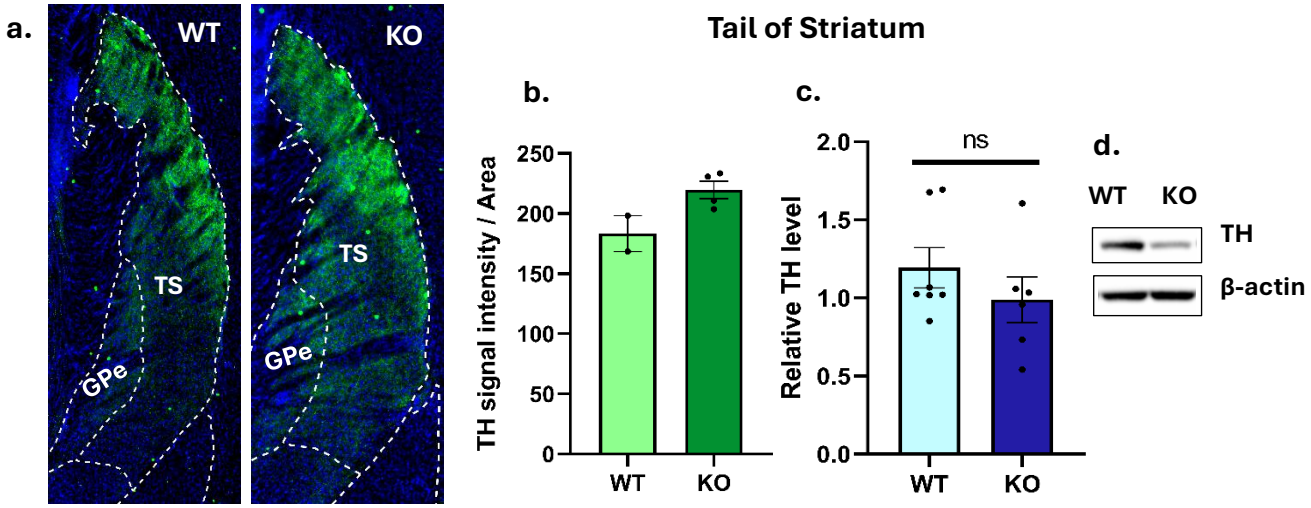


Figure 9 | Immunohistochemical staining of TH in the TS suggests a slight increase in *Shank3* KO mice but western blot data show no difference. a. Representative immunofluorescent images of coronal brain sections from WT (left) and KO (right) mice staining nuclei in blue and TH in green in the TS with 20x objective lens. **b.** Measured signal intensity of TH normalised for total area of TS. *(WT: n = 2 mice; KO: n = 4 mice)*. **c and d. Western Blot results.** Representative Western Blot of TH and β-actin bands in WT (left) and KO (right) brain tissue from the TS (**d.**) and quantification of TH signal normalised for β-actin (**c.**). *(WT: n = 7 mice; KO: n = 6 mice)*. Values presented as mean ± SEM. ns – no significant difference. Abbreviations: GPe, external *Globus Pallidus; TS, Tail of the Striatum*

Similarly to what happened with the data obtained for the SNpL, immunofluorescence results in the TS suggest a slight difference between genotypes, in this case as an increase in TH-stained signal in the *Shank3* KO mice compared to the WT group (Figure 9b.). This higher intensity could be perceived as a higher amount of TH expressed in the axons present in that area, but, same as before, western blot confirmation of these results leads to no statistically significant differences between groups, despite qualitative analysis of the western blot data suggesting a tendency for lower levels in the KO group.

3.4 D_1Rs may be less expressed in neurons of *Shank3* KO mice than in WT mice

After the release by the presynaptic neuron, dopamine relays the signal by acting upon postsynaptic dopamine receptors, therefore becoming the next focus of this study. As previously mentioned, the TS is mainly comprised of D_1R- and D_2RSPNs, which, in spite of being both involved in regulating threat-coping behaviours, play essentially contrasting roles. Given that D_1R-SPNs project directly into the *substantia nigra*, both the TS and SN domains were evaluated.

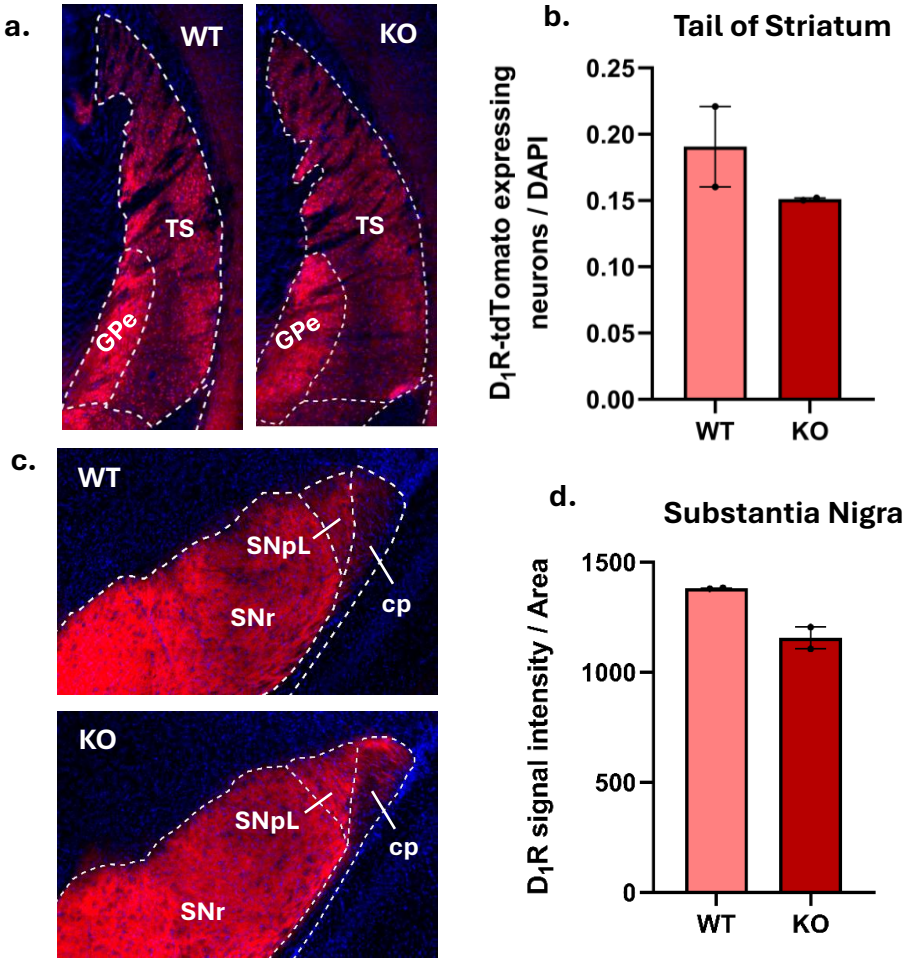


Figure 10 | Expression of tdTomato in the TS and SNpL suggests lower levels of D_1R in *Shank3* KO mice compared to WT mice. a. Representative images of coronal brain sections from WT (left) and KO (right) mice, showing DAPI staining in blue and D_1R-tdTomato signal in red in the TS with 20x objective lens. **b.** Number of D_1R-tdTomato-expressing cell bodies normalised for total number of DAPI nuclei in the TS. *(WT: n = 2 mice; KO: n = 2 mice)*. **c.** Representative images of coronal brain sections from WT (above) and KO (below) mice, showing DAPI staining in blue and D_1R-tdTomato signal in red in the SN with 20x objective lens. **d.** Measured signal intensity of D_1R-tdTomato normalised for total area of SNpL. *(WT: n = 2 mice; KO: n = 2 mice)*. Values presented as mean ± SEM. Abbreviations: cp, cerebral peduncle; GPe, external *Globus Pallidus*; SNpc, *Substantia Nigra pars Compacta*; SNpL, *Substantia Nigra pars Lateralis*; SNr, *Substantia Nigra pars Reticulata; TS, Tail of the Striatum*.

Akin to what was done for TH data, potential differences in D_1R-expressing neurons were assessed by fluorescence imaging through D_1R-tdTomato-expressing animals with the logging of individual cell body counts normalised for total number of DAPI nuclei in that TS area. Three slices per animal were averaged (Figures 10a. and b.), and mean signal intensity of D_1R-tdTomato-expressing axons in the SNpL was averaged across 3 different slices per animal (Figures 10c. and d.).

Of note, due to the reduced number of animals in each group, these preliminary results can't reliably undergo statistical analysis, and no definitive conclusions can be taken. However, there is a consistent tendency both in the TS and SNpL data for decreased tdTomato signal in *Shank3* KO mice compared to the WT group.

3.5 Administration of D_2R agonists lowers overall movement

Following the rationale of the previous section, D_2 receptors were the next logical territory to explore, however, due to practical constraints, it was not possible to perform further molecular biology experiments. Nevertheless, the downstream effects of dopamine pertaining to these receptors were still assessed by pharmacological modulation.

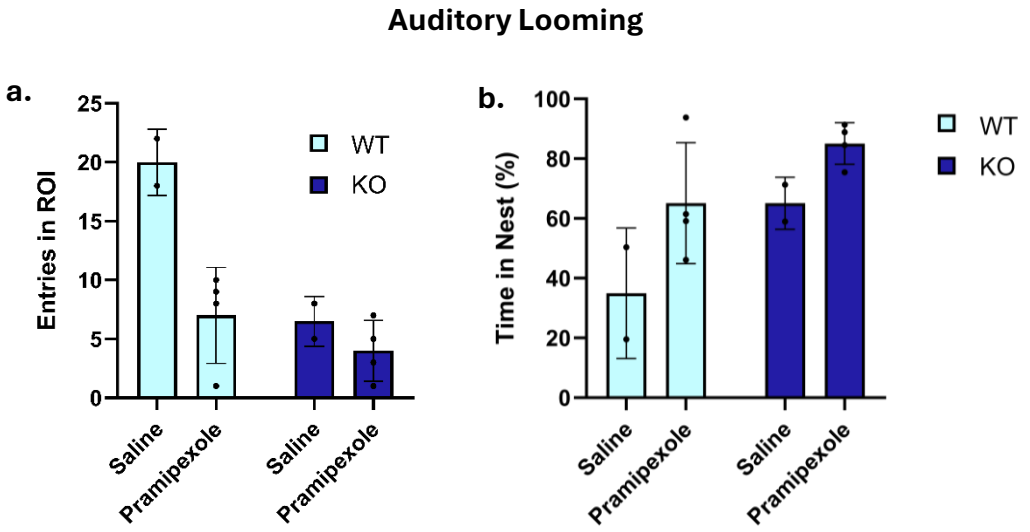


Figure 11 | Pramipexole-injected mice enter the sound area less often than saline injected mice and spend more time in the nest regardless of genotype. a. Number of times each WT and KO mouse entered the ROI during their trial of auditory looming behavioural test after being injected intraperitoneally with saline solution (left) *(WT: n = 2 mice; KO: n = 2 mice)* or D_2R agonist, pramipexole (right) *(WT: n = 4 mice; KO: n = 4 mice)*. **b.** Percentage of time each WT and KO mouse spent in their nest during each period of their trial of auditory looming behavioural test after being injected intraperitoneally with saline solution (left) *(WT: n = 2 mice; KO: n = 2 mice)* or D_2R agonist, pramipexole (right) *(WT: n = 4 mice; KO: n = 4 mice)*. Values presented as mean ± SEM.

Given D_2R-SPNs' functions regarding threat-avoidance behaviours, mice were intraperitoneally injected with either a D_2R agonist (pramipexole) solution at a concentration of 0.3mg/kg or a saline solution 1h before being subjected to the auditory looming paradigm to evaluate downstream behavioural readout in this task.

Results show that WT mice enter the ROI far less in the group injected with pramipexole compared to the saline injected group (Figure 11a.), a trend that can likewise be seen in the KO group, although to a lesser extent, and the amount of time spent in the nest also increased substantially upon pramipexole injections (Figure 11b.).

As such, to check if the decrease in number of entries in the ROI and locomotion could be due to pramipexole-induced motor impairments or an increase in anxiety in the mice, the same animals were observed in a home-cage behavioural analysis in which, after being injected intraperitoneally with the same solution as they had been in the previous trial, they were left inside their undisturbed enclosures with their cagemates for 10 minutes with only the top lid removed in as much silence as possible with no auditory stimuli being played. The time each individual mouse spent moving was manually counted (Figure 12).

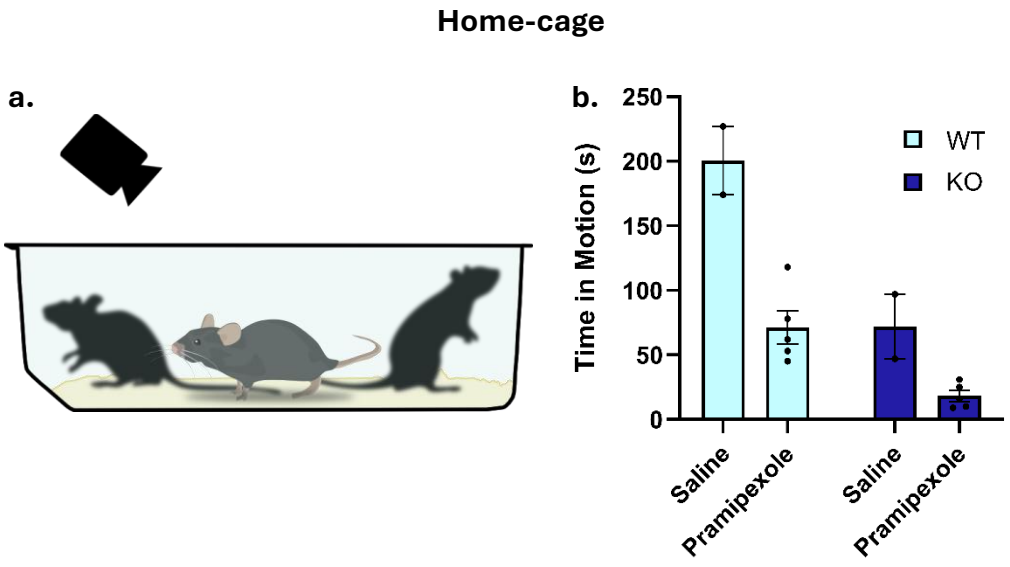


Figure 12 | Pramipexole-injected mice move less than saline-injected mice in home-cage test with no triggerable auditory stimulus. a. Diagram of home cage behavioural recording. Mice are placed in their original housing cages with their housing mates for 10 minutes while being recorded. **b.** Amount of time each individual mouse spent moving inside the cage after being injected intraperitoneally with saline solution *(WT: n = 2 mice; KO: n = 2 mice)* or D_2R agonist, pramipexole *(WT: n = 5 mice; KO: n = 5 mice)*. Values presented as mean ± SEM.

Despite the lack of external sources for predictable added anxiety, pramipexole-injected mice remained consistent with the previous test, displaying overall decreased locomotion in both genotypes (Figure 12b.). This can readily be attributed to the drug administration route as with a simple intraperitoneal injection, pramipexole is distributed systemically which means the acting site isn't specific, in this case leading to an activation of D_2Rs in all accessible brain regions.

Pramipexole effects have, in fact, been described as being dose dependent, and decreased locomotion and even sedation results are compatible with previous reports in literature of low doses of the drug by stimulating presynaptic D_2 autoreceptors which would explain the observed results, but this experiment could still see a turnaround by better optimising dosage and using brain-region-specific infusion as an administration option with techniques like cannula implantation in future iterations.

Discussion

- *THE SHANK3-INSG3680$^{(+/+)}$ MOUSE MODEL SHOWS AUDITORY AVOIDANCE IN MORE THAN ONE WAY*
- *TYROSINE HYDROXYLASE LEVELS DON'T SUPPORT A DOPAMINE SYNTHESIS INCREASE IN THE SNpL OR THE TS OF Shank3 KOs*
- *DOPAMINERGIC ACTION MAY BE ALTERED AT A RECEPTOR LEVEL IN Shank3 KO MICE*
- *DOPAMINE CLEARANCE MECHANISMS REMAIN UNEXPLORED*

4 | DISCUSSION

4.1 The *Shank3*-InsG3680$^{(+/+)}$ mouse model shows auditory avoidance in more than one way

This work set out to gauge the existence of any possible alterations to the SNpL-TS dopaminergic circuit in a *Shank3* KO mouse model of ASD, and whether such an alteration could be associated with this model's exaggerated auditory avoidance behaviour. The existence of the SNpL-TS circuit was aptly observed in the studied mice and the auditory looming paradigm, as described earlier, was used for simultaneous evaluation of anxiety-like behaviours and changes to locomotion on top of the avoidance behaviours. When exposed to this test, the KO mice entered the sound area less frequently than the WTs with no significant differences detected in their travelled distances or time spent in their nests, further supporting an auditory-avoidant phenotype.

Previous work had already established this *Shank3*-InsG3680$^{(+/+)}$ model as presenting auditory avoidance behaviours using a behavioural paradigm based on playing distinct continuous pure tones or falling to silence depending on the mouse's place in different areas of an arena[80]. Such a paradigm is fundamentally different from the one used in this study, particularly, in the fact that the auditory looming test is built around a crescendo, looping sound stimulus instead of a single, continuous one. In this case, the crescendo stimulus plays for as long as the animal remains within the ROI, resetting upon its exit. This detail draws more on the dynamic nature of a looming sound allowing for a more multidimensional assay of hyperacusis like the fear and annoyance aspects instead of simply the loudness aspect and, when conjugated with prior research, further strengthens the confidence in this model as one with auditory avoidance tendencies.

Interestingly, *Shank3* KO mice have been reported to display lower levels of locomotion in comparison to WT mice, and such results have been replicated by fellow members of the lab in their own experimental protocols, as well as observing a preference for their nest in behavioural tests. In this study, however, no statistically significant differences were found. Coincidentally, all previous reported findings to this regard were obtained from experiments where the mice were handled by female scientists, unlike the procedures carried out for this work. When handled by a male scientist, mice show higher levels of aversion to their scent as well as higher anxiety indicators which could create two opposing variables in the evaluated parameters. Increased levels of anxiety would lead to an expectation of the time mice spent in their nest to be higher, but since the nest was handled, set up, and placed inside the arena by the male handler as well as kept in one of the corners closest to the experimenter, the aversion to the lingering smell could have taken over and led the mice to move around more in an attempt to escape the stressful smell, counterbalancing the time they would otherwise have spent in their nests.

4.2 Tyrosine hydroxylase levels do not support a dopamine synthesis increase in the SN or the TS of *Shank3* KOs

The simplest prediction for a mechanism underlying exaggerated auditory avoidance in *Shank3* KO mice due to an excess in dopaminergic signalling would be that the rates of dopamine synthesis themselves be elevated in this genotype. As such, the rate-limiting enzyme involved in dopamine's synthesis pathway, tyrosine hydroxylase, became a relevant point of study available for this prediction, but the results obtained don't indicate any changes that could support it.

As the dopamine released in the TS is mostly released by the SNpL, it could be that there is a higher density of dopamine-producing TS-projecting neurons in that region, but immunohistochemistry analysis indicated a lower proportion of TH-expressing neurons in *Shank3* KO animals relative to WT. As such, it was plausible that a lower number of DA neurons could be compensated by an upregulation of synthesised dopamine, but western blot analysis of the same region showed no statistically significant genotype differences in pure TH quantities. These two results are not inherently as mutually exclusive as they may first appear for a few reasons. One such reason is the fact that the immunohistochemical quantification was restricted specifically to the SNpL area in the quantification software, whereas the tissue sampled for western blotting was obtained by macrodissection of the *substantia* nigra as a whole, which, as a biological sample, vastly outmatches the *pars lateralis* in size. That way, from the WB results alone, it can't be discarded that a SNpL-specific difference in dopamine synthesis could still be present but "diluted" to a point below detectable once averaged into a signal dominated by SNc-derived protein. Even so, it's relevant to keep in mind that the two methodologies are capturing different biological quantities as neuron soma counts reflect how many TH-positive cell bodies are present and not necessarily how much TH protein each of said neurons produces. Since these cells present in a lower number for the same amounts of TH, it may be that *Shank3* KO mice are producing proportionally more of the enzyme to match the levels observed in WT and that those alterations could have downstream effects that could be assessed in the following portion of the targeted circuit, the TS.

Immunohistochemical analysis of TH expression in the TS of the KOs suggest a non-significant increase in TH-expressing axonal signal but western blots of the same region have shown no significant differences in TH signal and, if a qualitative interpretation is to be given to the trend of expression, alterations actually leaned towards lower levels in the KO group, the opposite of what is shown by the IHC result. While the reduced number of animals used for IHC and the statistical insignificance in genotype-specific changes in TH expression in WB can't be ignored, one possible explanation for the opposite qualitative tendencies presented could lie in the lack of spatial-distribution sensitive information obtained by the WBs compared to IHC. The signal obtained in IHC conveys more than pure protein expression due to its sensitivity to the spatial arrangement of the target protein so it

could be possible that the same amount of TH is being expressed at a TS level as indicated by the WB results while also being more distributed in the same region, explaining the higher level of intensity detected by the IHC, despite being a theory that goes against previous research done *in vitro* in primary striatal dopaminergic neurons of a different type of *Shank3* KO mouse model[83] which report precisely a significantly reduced outgrowth of the neurites. As such the more direct explanation available is that the opposing trends may be a reflection of the limited statistical power of the immunohistochemical samples, leaving this specific comparison as unresolved.

Once again, such a conclusion does not necessarily rule out the possibility for altered dopaminergic signalling in this circuit however, in part because the methods used allow for a strictly anatomical assessment rather than a functional one. But posing the hypothesis that a different origin of dopaminergic dysregulation may stem not from a production baseline, but from the downstream action of dopamine after being synthesised and released in the way it interacts on its receptors.

4.3 Dopaminergic action may be altered at a receptor level in *Shank3* KO mice

The TH levels' results offered no clear support for a hypothesis of excess in dopamine synthesis in the SNpL-striatal circuit in this mouse model of autism, which resulted in a shift in attention towards the postsynaptic portion of the dopaminergic circuit. D_1R-SPNs are the population most directly linked in literature to driving avoidance responses with their activity preceding and promoting avoidance, while D_2R-SPNs activity facilitates the subsequent overcoming of a sustained threat instead[69]. Moreover, excessive pharmacological stimulation of D_1R-SPNs and the silencing of D_2R expression with siRNA in the dorsal striatum have both been linked to the promotion of typical autistic-like behaviours in mice[84] and so, given these findings, the working predictions that emerged were that *Shank3* KO mice could present elevated D_1R expression in the TS to explain their increased avoidance phenotype or that, conversely to the stimulation results of the D_1Rs, D_2R pharmacological activation could alleviate some of the avoidant tendencies, essentially leading to a shift in focus of the study to a receptor-centred level.

At face value, the obtained fluorescent data for D_1R associated with tdTomato's (D_1R-tdtomato) signal intensity oppose the first portion of the hypothesis with D_1R-tdTomato signal showcasing a qualitative tendency for lower levels in *Shank3* KO mice than in WT animals, consistently in both the TS and the SNpL. Nevertheless, lower receptor expression isn't necessarily linked to reduced dopaminergic activity especially since long-term exposure to dopamine has been shown to lead to a compensatory downregulation in dopamine receptor density[85]. As such, this reduction in D_1R expression may not be direct evidence against increased dopamine activity in the SNpL-TS circuit of *Shank3* KO mice but

rather, a downstream consequence of it as an adaptation to chronically higher levels of dopamine exposure. These results alone, however, aren't enough to extract a tangible conclusion and further studies regarding dopamine release and its way of action in dopamine receptors are necessary.

A different, opposing, role dopamine has been shown to play in threat-related conflicts arises from its action on D_2R-SPNs that, when activated, facilitate threat overcoming behaviours[69]. Therefore, if an altered dopamine pathway is underlying auditory avoidance behaviours in mice, it could be expected that activation of that same neuronal subpopulation would lead to a reduction in avoidance in the KO mice, bringing their performances on the auditory looming paradigm closer to the ones seen in the WT group. For that, mice were injected with a selective D_2R agonist, pramipexole, but the administration was done intraperitoneally, which proved to be a hindrance to the results obtained when the same mice were later assessed for locomotive impairments.

Beyond its actions on postsynaptic D_2R-SPNs, the drug also acts on presynaptic D_2 autoreceptors[86], which, when activated, suppress further dopamine synthesis and release from the presynaptic terminal in an autoinhibitory action[87] previously documented to result in sedation and hypomotility at low systemic doses[86]. A systemic administration, as what was performed, leads to pramipexole reaching D_2Rs throughout the entire brain rather than selectively within the TS, meaning that any behavioural changes that stem from it, reflect the sum of an activation in all D_2R-expressing populations and associated circuits. This is what the home-cage experiment was set to assess and, analysing the results, while it is true that the drop in motility was more pronounced between the subgroups of the WT mice compared to the ones of *Shank3* KO mice, any form of injection can be stressful for mice and, as such, the more likely explanation for the more subtle changes between the saline- and pramipexole-injected KO mice in locomotion is the existence of a floor effect in mice that are already particularly more anxious than their WT counterparts[88]. Thus, the only objective conclusion from this experimental procedure is that pramipexole-injected mice moved notably less than saline-injected mice for both genotypes in a context with no auditory stimulus and, therefore, no avoidance-relevant information could be obtained.

4.4 Dopamine clearance mechanisms remain unexplored

There's one more step in the lifecycle of a neurotransmitter worth exploring that keeps an altered dopaminergic system hypothesis from being discarded. After binding to a corresponding receptor in the postsynaptic cell, a neurotransmitter's action must have a way to be ceased to allow for another firing cycle to begin[89]. For catecholamines, such as dopamine, inactivation can be achieved mainly through reuptake by specific membrane proteins or, to a lesser extent, through enzymatic degradation by monoamine oxidases (MAOs) or catechol-o-methyltransferases (COMTs), though these usually occur when transporter activity isn't as available but, in the striatum, dopamine's activity is mainly terminated by the action of the dopamine transporter (DAT) on the presynaptic membrane[90].

That was meant to be the next exploratory step as described in the western blot portion of the Materials and Methods section but, unfortunately, the primary antibody acquired did not work and further optimisations are needed. However, this factor deserves its fair consideration mainly because it offers a mechanism that would reconcile and support the two central findings mentioned above without requiring either an increase in dopamine synthesis in the presynaptic neuron or an increase in receptor number in the postsynaptic neuron. If DAT-mediated reuptake were impaired or somehow reduced in the SNpL-TS circuit in *Shank3* KO mice, the dopamine released by the TS-projecting SNpL neurons would remain available in the synaptic cleft for longer, prolonging its action on the postsynaptic D_1R- and D_2R-SPNs before it is cleared, which would translate in a perceived higher signal in the downstream pathways. That would mean that, by all accounts, dopaminergic tonus in the TS could be functionally elevated due to higher receptor activation over time, without any corresponding upstream increase in the rate or amount of dopamine synthesised and released, proving consistent with the TH findings, and it would also point to the long-term dopamine exposure in the postsynaptic receptors expected to drive the compensatory D_1R downregulation theory discussed before.

Research done in Fmr1-KO mice has found, precisely, a decrease in striatal DAT expression levels compared to a WT strain[91]. It's important to note that that is a completely different model of autism so these findings don't hold much, if any, translational value, but effectively, they do set a precedent for altered expression related to reuptake mechanisms in an animal model that presents autistic-like traits which introduces some plausibility to this hypothesis as a worthy route to explore in the *Shank3* KO mice.

Final Remarks

- *LIMITATIONS*
- *FUTURE PERSPECTIVES*

5 | FINAL REMARKS

5.1 Limitations

The work developed in the context of this dissertation has set up a few avenues for future research but, before expanding upon those, it's important to address some of the limitations associated with the study as a whole.

One of the limitations that hindered a conclusive interpretation of the results obtained the most, has to do with the sample sizes. Besides the behavioural tests' results and the western blot quantifications of TH, the experiments done comprised of groups too small to perform reliable statistical analysis, resulting in mostly qualitative work and returning non-significant results for most of the evaluated domains but particularly for the immunohistochemical quantifications. The results obtained pertaining to those, indicate trends between genotypes but, at their current state, little to no concrete conclusions can be confidently ascertained.

On the topic of the IHC, the cell-density quantifications were normalised to the total number of DAPI-stained nuclei in the traced region, but DAPI as a stain, is not cell-type specific which meant the observed signal includes glial cell nuclei alongside neuronal nuclei. *Shank3* KO mice have had reports of region-specific microglial alterations before[92] so it's plausible that using that metric as a normalisation could introduce some unforeseen variability to the registered values. It must be stated that the brain slices were treated with a neuron-specific marker, NeuN, exactly for this purpose but that staining did not label reliably across all sections, which was the reason that led to ultimately using DAPI as the normalising metric.

There were a few further practical constraints that shaped which assessments could be completed as originally intended. First, due to technical limitations, pramipexole's administration was done systemically via intraperitoneal injection instead of locally into the TS, which, as discussed previously, compromised any firm interpretations to the D_2R-mediated behavioural modulations expected. Second, the primary antibody used for DAT detection did not yield a detectable signal and, due to time restraints, could not be replaced, which led to the abandonment of the experimental tackling of the reuptake domain in the dopaminergic pathway, arguably the most promising step to reconcile the seemingly unchanged TH signal with a functionally elevated dopaminergic tone. Antibody unavailability also introduced some reservations to the receptor focused strategies used, limiting possible confirmations of the IHC results or the attempt at more uniform methodological approaches for different biological variables like western blots for TH, D_1Rs and D_2Rs for the same animals.

Moreover, the initial proposal for this thesis' work plan set out to perform chemogenetic and optogenetic experiments in the SNpL-TS surrounding the dopaminergic circuitry. However, the first anatomical tracing experiments revealed through colocalization analysis of eYFP and TH labelling that a subset of eYFP-positive neurons were not TH-positive, indicating that a proper study of the SNpL-TS dopaminergic circuitry would require an added layer of specificity by using DAT-Cre mice, for example. For this reason, this study adopted a more generalised, fixed anatomical and biochemical approach rather than capturing the dynamic activity of the SNpL-TS circuit at the specific moments of auditory avoidance behaviours. Since the working hypothesis leans on an amplification of an auditory signal as it travels through this circuit, the dopaminergic differences in the KO mice, if present, may lie less in dopamine synthesis or quantities and distributions of receptors at rest, and more in the timing of dopamine release itself and subsequent evoked responses, neither of which can be aptly captured by a static endpoint. Nonetheless, these biochemical approaches remain a relevant and necessary starting point especially since they can be comparatively quick and the techniques are already established within the lab, which can help detect and direct the following approaches by pointing to routes that may be more worth exploring over others before committing fully to different techniques that may be more dynamic in nature but ultimately more costly both financially and timewise.

Finally, one major limitation worth addressing concerns how translational the anatomical framing adopted in this study really is. The TS is treated here as with the wider literature, as the rodent counterpart of the primate caudate tail (CDt), but the correspondence between the two is not absolute, especially in this auditory framework since the TS and the CDt don't share fully identical patterns of anatomical input[93] and, as such, may be involved in partially distinct sensory processing roles. Therefore, any conclusions drawn about the mouse TS can't be assumed to transfer fully and directly onto the human caudate tail without independent confirmation in a more closely matched model first.

5.2 Future Perspectives

In line with most of its limitations, there's still a lot of promising work to be developed regarding the experimental setups that emerged from this study. The most immediate priority is a replication of most of the experiments with a larger number of animals per group so that the comparisons that could only be treated qualitatively here, can be quantifiable and more confidently examined.

Besides an increase in n per group a further complement to the biochemical side of this analysis would be quantification of the examined proteins at a genetic level using strategies such as RT-qPCR for *TH*, *D_1R*, *D_2R*, and *DAT* genes in biological samples obtained from the TS and SNpL of WT and KO mice. Not only could these experiments help determine whether alterations to their expression are present from developmental stages or as the result of neuroplastic adaptations, but more specifically, it could also help resolve the aforementioned discrepancy between the immunohistochemical and western blot TH results by introducing another dimension of this protein's expression to be analysed.

The dopaminergic pharmacological modulation of D_2R-SPNs that has been previously established could also be explored at a more circuit-specific level by employing, as previously mentioned, the implantation of directed cannulas, targeting the TS. This way, D_2R- (or even D_1R-) specific drugs could be administered regionally and coupled with auditory looming tests to gauge more directly how different neuronal subpopulations influence avoidance behaviours, especially since local TS pharmacological modulation of dopamine receptors has already been successfully carried out in a different *Shank3* mutant line studied in a non-auditory context. A more direct test of how dopaminergic modulation of the TS is expressed in avoidance behaviours would be through a real time targeted strategy such as optogenetic manipulation of the SNpL neurons projecting to the TS, performed during the auditory looming paradigm itself. If neuronal activation of this region shifted the WT phenotype towards that of the KOs or an inactivation ameliorated the avoidance behaviours seen in the KOs by causing them to approximate to the WT phenotype, their role in these behaviours would be essentially confirmed leaving the underlying mechanisms to be further explored.

References:

Automatic citation updates are disabled. To see the bibliography, click Refresh in the Zotero tab.

FACULDADE DE **MEDICINA**